IEEE Access
Multidisciplinary | Rapid Review | Open Access Journal

Received August 1, 2019, accepted August 19, 2019, date of publication August 21, 2019, date of current version September 4, 2019.

Digital Object Identifier 10.1109/ACCESS.2019.2936789

Design Optimization and Model Predictive Control of a Standalone Hybrid Renewable Energy System: A Case Study on a Small Residential Load in Pakistan

HABIB UR RAHMAN HABIB[1,2], SHAORONG WANG[1], M. R. ELKADEEM[1,3], AND MAHMOUD F. ELMORSHEDY[1,3]

[1]School of Electrical and Electronics Engineering, Huazhong University of Science and Technology, Wuhan 430074, China
[2]Department of Electrical Engineering, Faculty of Electrical and Electronics Engineering, University of Engineering and Technology Taxila, Taxila 47050, Pakistan
[3]Electrical Power and Machines Engineering Department, Faculty of Engineering, Tanta University, Tanta 31512, Egypt

Corresponding author: Habib Ur Rahman Habib (hr_habib@hust.edu.cn)

This work was supported by the National Key Research and Development Program of China under Grant 2017YFB0902800.

ABSTRACT Renewable energy sources (RESs) offer a promising prospect for covering the fundamental needs of electricity for remote and isolated regions. To serve the customers with high power quality and reliability, design optimization methodology and a possible power management strategy (PMS) for wind-diesel-battery-converter hybrid renewable energy system (HRES) is proposed in this paper. The analysis is applied to a real case study of a standalone residential load located in a remote rural area in Pakistan. Firstly, optimal component sizing is investigated according to actual meteorological and load profile data. Different hybrid configurations are modeled, analyzed, and compared in terms of their technical, economic and environmental metrics with the aid of HOMER® software. The main objective is to determine the most feasible and cost-effective solution with least life-cycle cost, keeping in view the impact of carbon emissions. Secondly, a suitable PMS based on the state of charge (SOC) of the battery is proposed and implemented in MATLAB/Simulink® software for the designed HRES. The PMS is targeted to maintain load balance and extract maximum wind power while keeping the battery SOC within the safe range. Model predictive control (MPC) approach is applied to improve the output voltage profile and reduce the total harmonic distortion (THD). The boost converter is used for maximum power extraction from the wind. The DC-DC buck-boost battery controller is utilized to stabilize the DC bus voltage. The design optimization results show that the hybridization of wind, battery, and converter presents optimal configuration plan with minimum values of total net present cost (14,846 $) and cost of energy (0.309 $/kWh), which means 76.7% reduction in both total system cost and energy cost and 100% saving in harmful emissions when compared to the base case using diesel generator. The proposed system is able to support hundred percent of the load demand with excess energy of 30.1%. Performance analysis of PMS under variable load and fluctuating wind power generation is tested, and promising results with efficient load voltage profile is observed. Further, THD is reduced significantly to 0.26% as compared to 2.62% when the conventional PI controller is used. The output of this work is expected to open a new horizon for researchers, system planners for efficient design and utilization of HRES to curb drastic increase in load demand for urban as well as rural areas.

INDEX TERMS Hybrid renewable energy system, techno-economic optimization, power management strategy, model predictive control, residential load, net present cost, microgrid, HOMER® software.

NONCULTURE

ABBREVIATIONS

RES	Renewable energy source
RERs	Renewable energy resources
PMS	Power management strategy
SOC	State of charge
MPC	Model predictive control
MPVC	Model predictive voltage control
MPPT	Maximum power point tracking
HOMER	Hybrid optimization of multiple energy resources

The associate editor coordinating the review of this article and approving it for publication was Shuaihu Li.

LCC	Life cycle cost
COE	Cost of energy
HRES	Hybrid renewable energy systems
GHGE	Greenhouse gas emission
ESS	Energy storage system
DERs	Distributed energy resources
NPC	Net present cost

PARAMETERS, CONSTANTS, VARIABLES AND FUNCTIONS

ρ	Air density
R	Rotor blade radius
v_w	Wind speed
λ	Blade tip speed ratio
β	Pitch angle
C_p	Power coefficient
k_g	Gear ratio of gearbox
ω_t	Wind turbine rotational speed
ω_D	DFIG generator rotational speed
H_D	Inertia constant of the DFIG
C	Power capacity levels
Ah_{Bat}	Battery ampere-hour
Wh_{load}	Load watt-hour
V_{Bat}	Battery voltage
Wh_{night}	Night watt-hour
Wh_{day}	Day watt-hour
n_a	Number of autonomous days
η_B	Battery efficiency
V_o	Open circuit voltage
R_b	Battery internal resistance
I_b	Battery discharging current
K	Polarization voltage
Q	Battery capacity
A	Exponential voltage
B	Exponential capacity
D_{Bat}	Duty cycle
$C_{t,ann}$	Total annual cost ($)
CRF	Capital recovery factor
N	System lifetime (yr)
i	Real interest rate (%)
$E_{t,ann}$	Total annual served load (kWh/yr)
P_{mec}	Mechanical power from the wind
PE	Power electronic
DOD	Depth of discharge
$O\&M$	Operating and maintenance

I. INTRODUCTION

The modern world is still struggling hard for harvesting maximum renewable energy sources (RESs) to compensate for the drawbacks of conventional energy resources due to greenhouse gas emissions (GHGEs), costly grid extensions, unserved remote areas, voltage quality issues, and distribution power losses. Table 1 shows typical renewable generation capacity utilized for small remote residential loads [1].

Due to high household consumption and industrialization, the drastic increase in energy demand requires more penetration of renewables to fulfill energy gap between suppliers and prosumers. Billions of peoples have no access to electricity, of which more than 80% are in rural areas [1]. According to the energy report addressed by United Nations in 2014, around 17.8% of the world population has no access to electricity [2]. Moreover, the last decade data shows 40% of total energy is used in buildings which is recorded as the large consumption globally [3]. Conventional energy sources being scarce and emit hazards gases [4] which are the major factors for climate change [5]. Furthermore, cities are the major contributors to anthropogenic greenhouse gases by about 65-75% [5]. To add with, grid blackout is often caused by natural disasters, while conventional resources (diesel, gas) are not capable of handling these worst-case scenarios [5].

Keeping the above issues in mind, conventional and centralized energy sources can be subsequently replaced with the RESs to simultaneously improve the technical and economic as well as the social metrics of the energy system ([2]. However, the individual use of RES brings unreliability and low-security issues and relatively increase the system cost. Therefore, hybrid renewable energy system (HRES) can be used as a sustainable, reliable, low-carbon and cost-effective solution to supply the load demand [5]. HRES can be defined as a combination of renewable energy resources (such as, photovoltaic (PV), wind turbine (WT), fuel cell (FC), hydro, etc.) and conventional (such as, diesel generator (DG), microturbine) equipped with energy storage systems that are used to supply electrical load demand in reliable, economic and environmental manners, either in grid-connected or grid-isolated modes [6]–[8]. To achieve the highest benefits from HRERs, the system has to be optimally designed and planned. Also, implementation of adequate and suitable power management (PMS) of HRES is a key necessity to ensure that maximum amount of energy is extracted from RESs.

In last years, the data shows rapid growth and high reliability in the technology of wind energy system [9]. Fig.1 shows the global trend in wind energy investment [10]. Each coming year brings wind installation with low levelized energy cost at an affordable price with less execution time even for standalone hybrid systems [9]. This has pushed researchers towards the feasibility analysis of applicability of WT generators, particularly in those windy residential areas where grid extension is not available, while peoples are still living without electricity. Therefore, Pakistan is looking towards the development of RE in the coming time. Pakistan is abundant in RE due to its strategic location [11] and has high potential of wind power generation [12]. Installed wind capacity in Pakistan is 1,448.2 MW at twenty-nine different locations while conventional resources have 24,823 MW (67.74% share of total electricity) installed capacity [11]. According to [12], current power shortage in Pakistan can be effectively resolved by increasing the share of WT and PV generators.

The rest of the paper is organized as follows: literature review is elaborated in section II while proposed approach is briefly discussed in section III and details for optimal design of HRES is presented in section IV. Control and

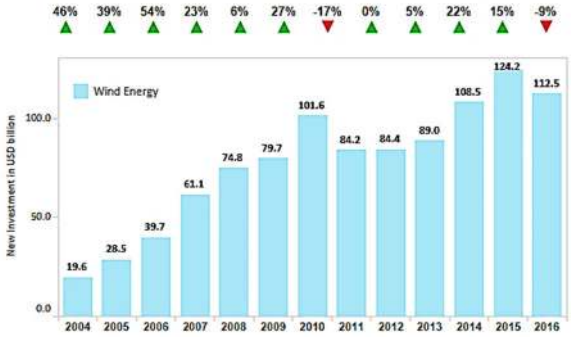

FIGURE 1. Global trends in wind energy investment [10].

TABLE 1. Renewable generation capacity [1].

Type	Size	Typical load
Large	> 100 kW	Regional loads
Medium	5 kW up to 100 kW	Isolated off-grid communities
Small	< 5 kW	Remote households

PMS of the designed HRES is presented in section V. Real case study and system description of the developed HRES is given in section VI. Simulation results and detailed results are introduced in section VII. Comparison between proposed system features with results and literature is investigated in section VIII. Finally, conclusions and main highlights are given in section IX.

II. RESEARCH BACKGROUND

So far, many researches have been investigated in the literature to study the topic of standalone HRES for remote area electrification. In [5], PV-WT-biomass-battery system is investigated for an urban area in Canada. PV-DG-battery standalone system of Tanzania is taken in [13]. PV-wind is considered in [14] for Algeria. PV-WT-battery is implemented for rural area electrification in India [4]. PV-WT-battery is studied by [15] for feeding small factory load located in a tropical island. Residential loads of six small cities of Nigeria are electrified with DG-WT-PV-battery system [9]. PV-biomass-DG system for rural area electrification in India is studied by [16]. PV-WT-biomass-battery with zero-emission and biochar production is proposed for a remote area in Philippines [17]. To fulfill electricity, thermal and hydrogen requirements, PV-WT-DG-battery-boiler-electrolyzer is used [18]. PV-WT-battery with hydrogen storage is used, and economic model predictive control (MPC) with outer sizing loop using genetic algorithm and inner PMS loop using mixed integer linear programming is proposed in [19]. PV-WT-battery is studied and observed that a smaller wind turbine unit (2kW) is the most suitable option for designing hybrid energy systems with the wind-alone system as more efficient as compared to the solar-alone system [20]. PV-WT-battery system is investigated with a focus on cost and reliability. Another study found that wind turbine size has no impact on results [21]. For pumping and desalination, PV-FC hybrid system in Egypt is compared with diesel only and grid extension. It is analyzed that the proposed system is cost-effective than grid extension [22]. PV-DG-battery system is proposed for Algeria [23]. A wind farm with biomass energy is designed in Iran. Agriculture wastes are used for biomass energy. This standalone system with 1.5MW capacity can be used as a grid-connected as well as standalone systems [24]. PV-WT-DG-biomass-battery is proposed, and PV-biomass-DG-battery is found to be an optimal solution [2]. PV-wind-diesel-battery is used and renewable share is increased from 68.5% to 81.4% [25]. PV-WT-hydro-biomass system is proposed for a rural area in India by using a logistic growth model for future demand calculation. Results show that increased generation with the constant annual cost is possible without significant effect on the environment [26]. PV-WT-DG-battery system for small community load (3.9kW peak load) in Malaysia is proposed in [27] with high energy cost (1.877$/kWh). PV-WT-FC residential system with seasonal and regular homes in Turkey is studied [28] with high energy cost. It is depicted that battery storage system is still superior to hydrogen storage technology. In [29], PI-based control with only battery SOC is briefly analyzed. Egyptian territory is chosen in [7] to compare different heuristic optimization techniques such as particle swarm optimization and genetic algorithm with HOMER software for optimal component sizing of the HRES with multiple sources (PV-WT-DG-gas-bio-battery). It is learned that PV and natural gas turbines can reduce the cost of energy than biomass generator. Moreover, biomass generator-battery combination can reduce GHGEs more than PV-gas turbine- hybrid energy system. Combined dispatch strategy for PV-DG-battery based rural electrification in Iraq is implemented in [30] and compared with load following and cycle charging scenarios. From the literature, most of paper that have been separately investigated the topics of HRES design optimization and power management and control of such systems, which is not practical and can lead to unfair results and misconclusions.

In this paper, the optimal design and plan of HRES has been determined and most proper and advanced PMS has been proposed. Firstly, the design optimization of HRES has been carried out based on comprehensive techno-economic simulation and optimization analysis for different hybridization scenarios of wind, diesel, battery and converter technologies. The developed HRES was used to meet the energy requirement of a standalone residential application located in Pakistan considering the practical load demand data and real-time weather data. Secondly, a self-made simulation tool has been developed with the aid of MATLAB/Simulink®to implement the proposed PMS. The PMS has been applied on the optimized system plan and successfully improve the system performance in terms of power quality, system stability under steady state and transient conditions of wind speed variation and abrupt load changes.

The key contributions of this paper are:

- An integrated and generic approach of optimal components sizing and energy flow control and management of stand-alone HRES is proposed. The suggested approach is demonstrated with a real case study for electrification of a small residential load located in a remote rural area in Pakistan.
- Feasibility study based on techno-economic simulation and optimization analysis for WT-DG-battery-converter based hybrid energy system is performed with the aid of HOMER® software in order to find the optimal HRES configuration (i.e. winning plan). with least cost and realistic environmental emissions. To achieve that, minimizing total net present cost (NPC) and levelized cost of energy (COE) as well as improving system reliability are incorporated in the objective function.
- An adequate and proper PMS is designed and verified by means of a self-made simulation tool developed in MATLAB/Simulink® software. The developed PMS is based on SOC of the battery and aim to maintain load balance and extract maximum power from the winning HRES and stabilizing constant AC bus voltage during wind speed fluctuations and abrupt load changes, meanwhile keeping the battery SOC within the allowable limits.

III. PROPOSED APPROACH FOR HRES DESIGN AND ENERGY MANAGEMENT

The proposed integrated and generic approach of optimal components sizing and energy flow control and management of stand-alone HRES is proposed as shown in Fig. 2. Initially, real-time meteorological data, which includes wind speed, temperature of specified location and load profile is assessed. After defining optimization objectives with constraints, possible configurations of the hybrid energy system, detailed modeling of various system devices is executed. Based on comprehensive techno-economic simulation and optimization analysis, the most feasible and optimal solution (i.e. wining configuration plan) for the proposed location is suggested and its technical, economic and environmental performance are assessed. After that, proposed PMS is executed for the winning plan. Finally, validation of suggested management strategy and their comparison with conventional ones is analyzed.

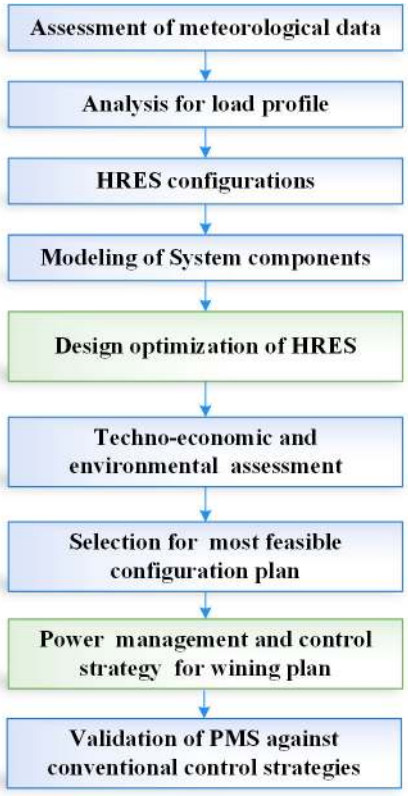

FIGURE 2. Proposed strategy for standalone system design optimization and energy management.

IV. DESIGN OPTIMIZATION OF HRES

In this section, a description of the developed HRES along with the detailed modelling of various system components is presented.

A. HRES STRUCTURE

Overall schematic diagram of the proposed HRES structure including the flow of control signal between various subs-systems is shown in Fig. 2. The proposed system is composed of WT, DG, and battery energy storage and power converter. WT and DG are used as the available primary sources to meet the load demand. The battery bank is used to supply power to the load during insufficient wind generation as well as under transients, ripples, and spikes. The system converter is essential to convert the DC electricity to AC between AC and DC buses and vice versa. It should be necessary to mention that the wind boost converter is designed for maximum wind power extraction while battery converter is used for stabilizing constant DC bus voltage.

B. MODELING OF THE DEVELOPED HRES

Recently, HOMER® software optimization tool, which is developed by National Renewable Energy Laboratory (NREL), USA [31] has been used in countless studies for optimization of different configurations of HRESs (e.g. PV/WT/Biomass/Battery/Converter [5],DG/PV/WT/Battery/Converter [9], [32], WT/PV/Battery/Converter [4], [33], PV/Biomass gasifier/DG /Battery/Converter [16], PV/WT/DG/Battery/Converter [31] PV-battery [34], PV/DG/ battery/Converter [23], PV-WT [14], [35], [36], only PV [37], [38], PV/Hydro/DG/Battery/Converter [39], PV-WT-battery/FC [3], [40]–[42]) for electrification of rural [4], [16], [35], [40] and urban [5], [9], [32], [36] areas with country-based study cases [4], [5], [38], [40], [9], [13], [14], [16], [32], [35]–[37] either for grid-connected [3], [13], [42]–[44], [16], [34]–[38], [40], [41], [45] or stand-alone [4], [5], [9], [13]–[16], [40] systems.

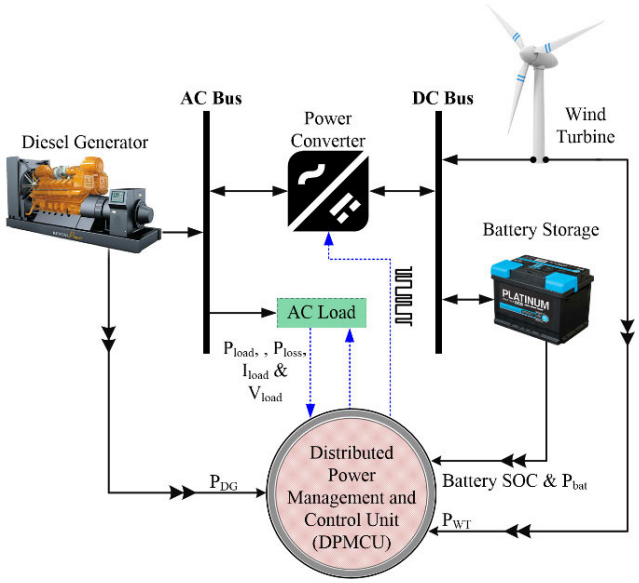

FIGURE 3. Proposed HRES schematic diagram.

HOMER fundamentally is a robust techno-economic optimization model [9]. It provides flexibility for techno-economic modeling and simulation analysis as well as design optimization of HRES components [9]. HOMER's optimization algorithms allow the designer and decision makers to evaluate the economic and technical feasibility of a large number of technology options considering the variations in technology costs and energy resource availability. Therefore, HOMER was chosen in this paper to perform feasibility and techno-economic design optimization of HRES to find the most viable and optimal configuration plan for supplying the investigated area.

1) WIND ENENRGY SYSYTEM

Components of wind generation are wind turbine, PMSG, and maximum power extraction mechanism. In this paper, WT model of the fixed pitch with variable speed is used, where the utilized model type was Xzer2.5 with a rated power of 2.4 kW, hub height of 30 m, cut-in and cut-out speeds of 2.2 m/s and 13.9 m/s respectively. Capital and replacement costs are assumed 5,000 $/kW [27] with operating and maintenance (O&M) cost as 40 $/kW. The lifetime of the selected turbine was 20 year. Wind mechanical power P_{mec}, is expressed as [46]:

$$P_{mec} = \frac{1}{2} C_p(\lambda, \beta) \rho \pi R^2 v_w^3 \tag{1}$$

The expression of Cp is defined as

$$C_p = 0.22 \left(\frac{116}{\lambda_i} - 0.4\beta - 5 \right) e^{-12.5/\lambda} \tag{2}$$

where

$$\lambda_i = \frac{1}{\frac{1}{(\lambda + 0.08\beta)} - \frac{0.035}{(\beta^3 + 1)}} \tag{3}$$

The blade tip speed ratio is given by

$$\lambda = \frac{\omega_t . R}{v_w} = \frac{k_g . \omega_D . R}{v_w} \tag{4}$$

Generally, the pitch angle will be set to zero when the value of P_{mec} is below the rated of power. Hence, Cp is the function of λ only and is maximum C_{pmax} at specific value of λ. At this stage, the WT attains the maximum power and the optimal rotor speed ω_{Dopt} for a specified v_w from (4). Substituting (4) in (1), yields:

$$P_{MPPT}^{WG} = \frac{\rho \pi R^5 k_g^3 C_{p\max}}{2\lambda^3} . \omega_D^3 = C_M . \omega_D^3 \tag{5}$$

Both the maximum power point tracking (MPPT) algorithm and the pitch angle control are simulated to regulate the active power of a WG. The reference active power is calculated by using MPPT model according to the current rotor speed (ω_D). The rotor motion equation to automatically reach optimal rotor speed is as follows:

$$2H_D . \omega_D . \frac{d\omega_D}{dt} = P_{mec} - P_{MPPT}^{WG} \tag{6}$$

Due to the fast response of power electronics devices, the active power from WT is considered as the same as the reference value of its power.

2) BATTERY ENERGY STORAGE SYSTEM

Battery backup is essential part of HRES to maintain system reliability, especially during the night and unwinds weather. SPRE 06 415 battery model was used in this study. The selected battery has 2.45 kWh nominal capacity, roundtrip efficiency of 80% and lifetime (throughput) of 1,958 kWh. The capital cost and replacement cost were supposed to be 176 $/unit, while O&M cost was 8 $/yr [28]. The minimum SOC of battery was 20%, and the maximum value was 80%. Deep cycle battery is used to bear discharge up to 20 % (DoD), and it is capable of fast charging. Battery size calculation can be determined as follows.

$$Ah_{bat} = \frac{Wh_{load}}{(DoD).(V_{bat})} \tag{7}$$

$$Wh_{load} = \frac{Wh_{night}}{\eta_B} + \frac{\left(Wh_{day} + Wh_{night}\right) . n_a}{\eta_B} \tag{8}$$

Figure 4 shows the battery controller while the battery charging and discharging can be controlled to stabilize load voltage and frequency [47]. The equations for the battery terminal voltage and SOC are as follows [48].

$$V_{Bat} = V_o - i_b R_b - K \frac{Q}{Q - \int i_b dt} + A e^{(-B \int i_b dt)} \tag{9}$$

$$SOC = 100 \left(1 - \frac{\int i_b dt}{Q} \right) \tag{10}$$

Battery SOC constraints are [48].

$$20 \leq SOC \leq 80 \tag{11}$$

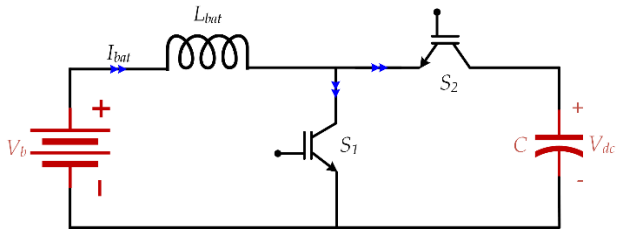

FIGURE 4. Battery controller.

$$-\frac{P_{Bat}}{V_{Bat}} \leq I_{Bat} \leq \frac{P_{Bat}}{V_{Bat}} \tag{12}$$

where P_{bat} and V_{bat} are battery rated power and nominal voltage, respectively.

Conventional droop control [49] for the battery is used. Battery inductor (L_{bat}) is designed according to the following relationship [50].

$$L_{Bat} = \frac{V_{DC}(1-D)}{2.f_{\min}.\Delta I_B} \tag{13}$$

3) POWER CONVERTER

The interlinking converter is used for exchanging power between AC and DC buses. The utilized converter has capital and replacement costs of 200 $/kW and zero O&M cost [27]. The chosen converter has a lifetime of 15 years and an efficiency of 95%. Power capacity levels of the converter can be determined according to the following equation.

$$C = (3 \times L_i) + L_r \tag{14}$$

where L_i and L_r are inductive and resistive loads. AC side mathematical model for inverter voltage vector is [48]:

$$V_i = V_g + R_f I_f + L_f \frac{dI_f}{dt} \tag{15}$$

where V_g, R_f, I_f, L_f are grid side load voltage vector, filter resistance, inverter output current, and filter inductance respectively. Inverter powers are related as [48]:

$$P = \mathrm{Re}\{V_g I_f\} = \frac{3}{2}\left(V_{g\alpha} I_{f\alpha} + V_{g\beta} I_{f\beta}\right) \tag{16}$$

$$Q = \mathrm{Im}\{V_g I_f\} = \frac{3}{2}\left(V_{g\beta} I_{f\alpha} - V_{g\alpha} I_{f\beta}\right) \tag{17}$$

LC Filter equation and inverter model with capacitor voltage V_c and load current I_L are expressed as follows:

$$C_f \frac{dV_c}{dt} = I_f - I_L \tag{18}$$

$$V_i = R_f I_f + L_f \frac{dI_f}{dt} + V_c \tag{19}$$

4) DIESEL GENERATOR

A diesel generator is used as a backup source during extreme demand to fulfill power deficit during high load consumption. Installation cost was 1000 $/kW, while O&M cost was 0.05 $/kW [7]. The price of diesel fuel per one Liter was supposed to be 0.8$ according to the market of Pakistan.

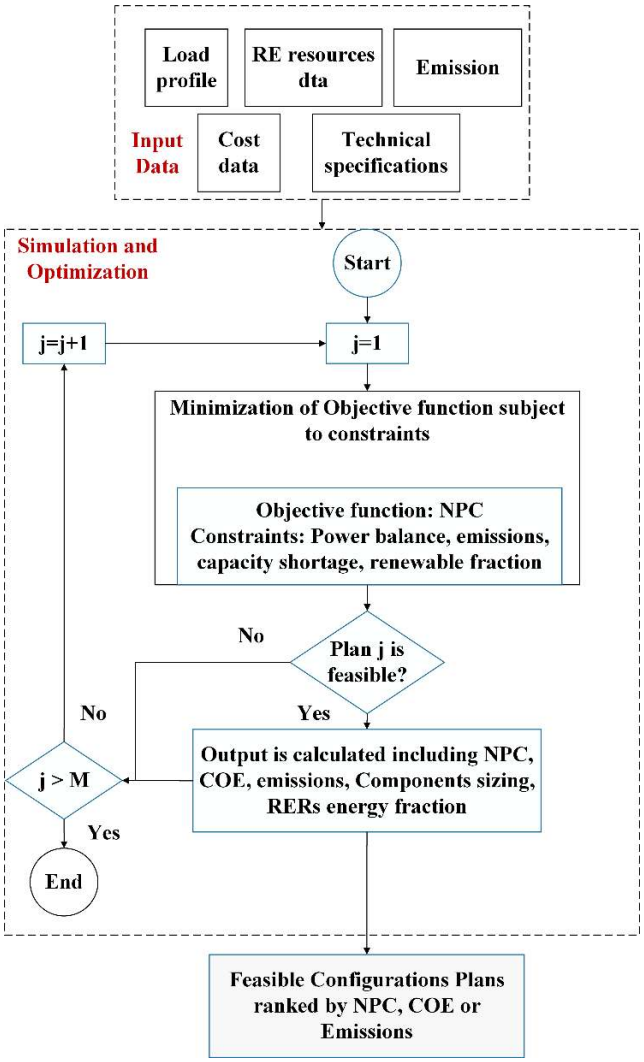

FIGURE 5. Applied methodology for HRES simulation and optimization analysis.

The lifetime of the diesel was 10000 hours with the minimum load ratio of the diesel generator was 25%. The diesel fuel consumption basically depends on the DG output power, and it can be calculated as follows [7]:

$$Fuel_{c,DG} = a.P_{DG,n} + b.P_{DG,g} \tag{20}$$

where, $Fuel_{C,DG}$ is the fuel consumption rate (L/h), $P_{DG,n}$ and $P_{DG,g}$ are the nominal power and generated power of the DG (kW), while a (0.0140 L/kW/hr) and b (0.2440 L/kWh/hr) are the coefficients of the diesel fuel consumption curve.

C. TECHNO-ECONOMIC DESIGN OPTIMIZATION OF HRES

Out of many possible combinations, HOMER provides fast and easy evaluation of optimal configuration. Figure 5 shows the applied optimization framework in this study. HOMER optimizes sizes of number of WTs, number of batteries pack, size of diesel generator, and size of power converters [4] based on load demand, resources data with economic,

technical specifications of each component, design constraints, applied control strategy and emission data as inputs [4], [9] and total NPC as an optimization objective [9]. HOMER provides one-year optimization analysis to evaluate the technical, economic and environmental performance of HRES [13], then all costs are extrapolated for the other years over the project lifetime based on linear depreciation method with best possible configurations that ensure continuous supply-demand balance on an hourly basis [9]. After testing all possible configurations of HRES, a list of feasible configurations can be obtained and ranked based on the design objective.

1) ECONOMIC MODELING

From the literature, different evaluation criteria have been presented to determine the optimal design of HRES. Most of these indices were based on specific economic factors such as NPC (also called life cycle cost), levelized cost of energy, system total cost, system annualized cost, average generation cost, etc. In this paper, minimization of total NPC and COE are the main objective of the optimization problem which can be expressed as follows [4]:

$$NPC = \frac{C_{t,ann}}{CRF(i,N)} \tag{21}$$

$$CRF = \frac{i(i+1)^N}{i(i+1)^N + 1} \tag{22}$$

$$COE = \frac{C_{t,ann}}{E_{t,ann}} \tag{23}$$

$$i = \frac{i-f}{1+1} \tag{24}$$

where, $C_{t,ann}$ is the total system annualized cost ($/yr) and *CRF (i, N)* is the capital recovery factor, *i, f* and *N* are the annual interest rate (%), inflation rate (%) and lifetime of the project (yr), respectively and $E_{t,ann}$ is the total electrical load served (kWh/yr).

Furthermore, the renewable fraction (RF) was considered as a valuable metric to measure the share of renewable energy source in the total energy supplied for the load. RF is defined as the fraction of the energy delivered to the load that originated from renewable power sources and can be expressed as follows:

$$\%RF = (1 - \frac{E_{non-ren,ann}}{E_{t,ann}}) \times 100 \tag{25}$$

where $E_{non-ren,ann}$ is the total annual non-renewable electrical production (kWh/yr)

2) DESIGN CONSTRAINTS

From Technical perspective, power balance and battery charge constraints can be expressed as in Eq. (24) [44], where Summation of consumed power should be equal or less than the maximum generated power from available energy sources.

$$\sum_{j=1}^{N} P_{WT} + P_{diesel} + P_{bat} - P_{load} = 0 \tag{26}$$

where P_{WT} shows the output power of i^{th} wind turbine unit and P_{diesel} represents the diesel output power. P_{bat} depicts the battery output power, If P_{bat} is positive, the battery is discharging and P_{bat} is negative during the charging mode.

Also, the power limits of generating units [44] and battery operation limits [44] should be satisfied.

$$P_{ch\arg e}^{\max} \le P_{bat} \le P_{disch\arg e}^{\max} \tag{27}$$

where, $P_{charge}{}^{max}$ and $P_{discharge}{}^{max}$ represents the maximum charging and discharging power of the battery.

From an environmental perspective, diesel generator produces harmful gases out of which carbon dioxide is the major contributor in emissions. Therefore, calculation of penalty cost of carbon dioxide emission is considered in the proposed system, which is [2].

$$CO_{2W} = \frac{C_C.E_{DG}}{1016.04} \tag{28}$$

$$CO_2 = \left(\frac{E_{TRC}}{C_C}\right).1016.04 \tag{29}$$

$$P_C = CO_{2W}.CO \tag{30}$$

where P_C, C_C, CO_{2W}, $ETRC$ are emission cost, the carbon content in kg/kWh, carbon weight in tons, and renewable cost in $/kWh respectively.

V. POWER MANAGEMENT STRATEGY

Model predictive voltage control (MPVC) is applied to control interlinking inverter for constant load voltage magnitude and frequency. DC-DC buck-boost battery converter controls DC bus voltage while wind boost converter is used to extract maximum power from wind. The following section explained all control and management strategies step by step.

A. MODEL PREDICTIVE CONTROL FOR INTERLINKING INVERTER

Working principle and MPC control strategy [51] are discussed in the following sections.

1) FCS-MPC PRIMARY CONTROL

By using Clark transformation, abc reference voltage signals are converted to α-β for the design of primary control. These reference values are then fed to the inner loop. RLC filter measurements (capacitor voltage and inductor current) are taken afterward to provide SVPWM gating signals to the interlinking inverter (VSI).

2) PRIMARY DROOP CONTROL

Filter Measurements (current and voltage) are used to find instantaneous active, and reactive powers, and finally, fundamental active and reactive powers are calculated. To properly control power-sharing and energy flow, droop strategy

(P–V/Q-ω) is applied for regulation of reference load voltage and frequency.

3) SINUSOIDAL REFERENCE GENERATOR

The three-phase sinusoidal generator is used to generate final reference signals to the inverter for voltage and frequency control.

4) INNER LOOP CONTROL

Continuous state space model for the three-phase interlinking inverter is designed in discrete time state space model by using RLC filter parameters. MPC based optimization algorithm find predicted voltage values for all sixteen combinations at next (t + 1) sampling time.

Continuous state space model of the above two equations is

$$\frac{dx}{dt} = Ax + By \tag{31}$$

To find the voltage at the next sampling instant, discrete state space modeling is calculated as

$$x(k+1) = e^{T_s.A}.x(k) + A^{-1}.(e^{T_s.A} - I_{2X2}).B.y(k) \tag{32}$$

By solving this equation for the discrete model, we get

$$\begin{bmatrix} V_{cj} \\ I_{fj} \end{bmatrix}^{k+1} = A_d \begin{bmatrix} V_{cj} \\ I_{fj} \end{bmatrix}^{k} + B_d \begin{bmatrix} V_{ij} \\ I_{oj} \end{bmatrix}, \quad for\ j = \alpha, \beta \tag{33}$$

$$A_d = e^{T_s A}, \quad B_d = \frac{B}{A}(A_d - I_{2X2}) \tag{34}$$

where Vi is voltage vector having eight switching states for converter switches (Sa, Sb, Sc) with the following the expression

$$V_i = \begin{bmatrix} S_a V_{dc} - \left(\frac{S_a+S_b+S_c}{3}\right) V_{dc} \\ S_b V_{dc} - \left(\frac{S_a+S_b+S_c}{3}\right) V_{dc} \\ S_c V_{dc} - \left(\frac{S_a+S_b+S_c}{3}\right) V_{dc} \end{bmatrix} = \begin{bmatrix} V_a - V_n \\ V_b - V_n \\ V_c - V_n \end{bmatrix} = \begin{bmatrix} V_{an} \\ V_{bn} \\ V_{cn} \end{bmatrix}$$

$$= \begin{cases} \frac{2}{3} V_{dc} e^{j(i-1)\frac{\pi}{3}} & for\ i = 1, 2, \ldots 6 \\ 0 & for\ i = 0, 7 \end{cases} \tag{35}$$

The cost function is then written as follows:

$$g_v = \sum_{j=1}^{n} \left[(V_{c\alpha}^{ref} - V_{c\alpha}^{k+j})^2 + V_{c\beta}^{ref} - V_{c\beta}^{k+j})^2 \right] \tag{36}$$

Cost function minimizes the difference between reference and predicted capacitor output voltage vectors in each iteration.

All possible eight switching states are used in the discrete model to minimize voltage error/difference (cost function) between reference and predicted voltage values for all eight possible states. Finally, one optimal cost function is selected, and the corresponding voltage vector is applied to IGBT switches of VSI.

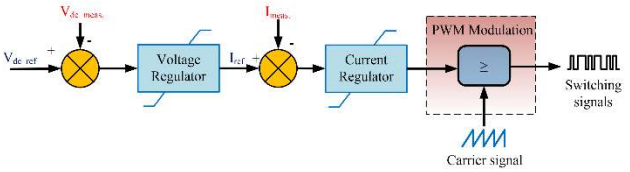

FIGURE 6. DC bus controller.

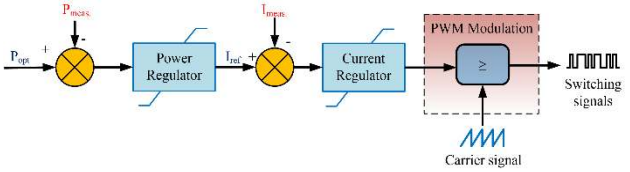

FIGURE 7. Controller for maximum wind power extraction.

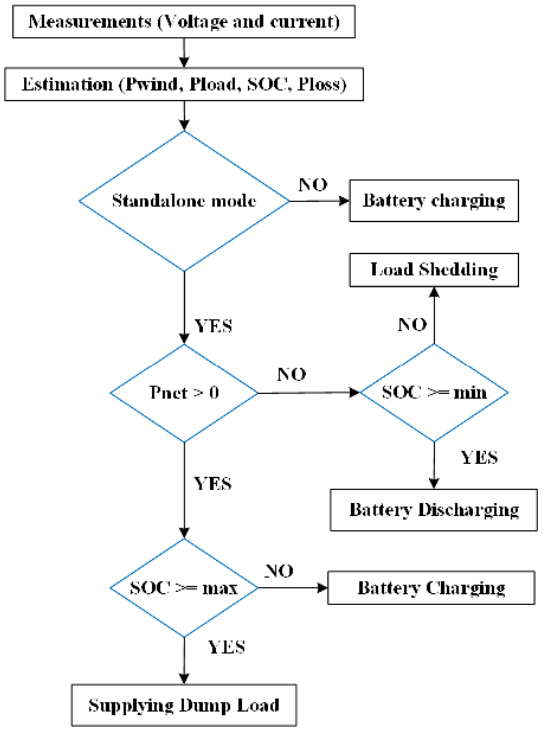

FIGURE 8. Applied power management strategy.

B. DC LINK VOLTAGE CONTROL

Battery controller (see Fig.6) for buck-boost operation is used to regulate dc bus voltage.

C. MAXIMUM WIND POWER EXTRACTION THROUGH WIND CONVERTER

Wind generator of the fixed pitch with variable speed is used in this study. Parameters of PMSG and wind turbine are taken from [52], with MPP controller as shown in Fig.7.

D. LOAD VOLTAGE AND FREQUENCY CONTROL

DERs in ac microgrid control active and reactive power based on the following droop equations

$$\omega_i = \omega_{nom} - m_i P_i \tag{37}$$

$$V_i = V_{nom} - n_i Q_i \tag{38}$$

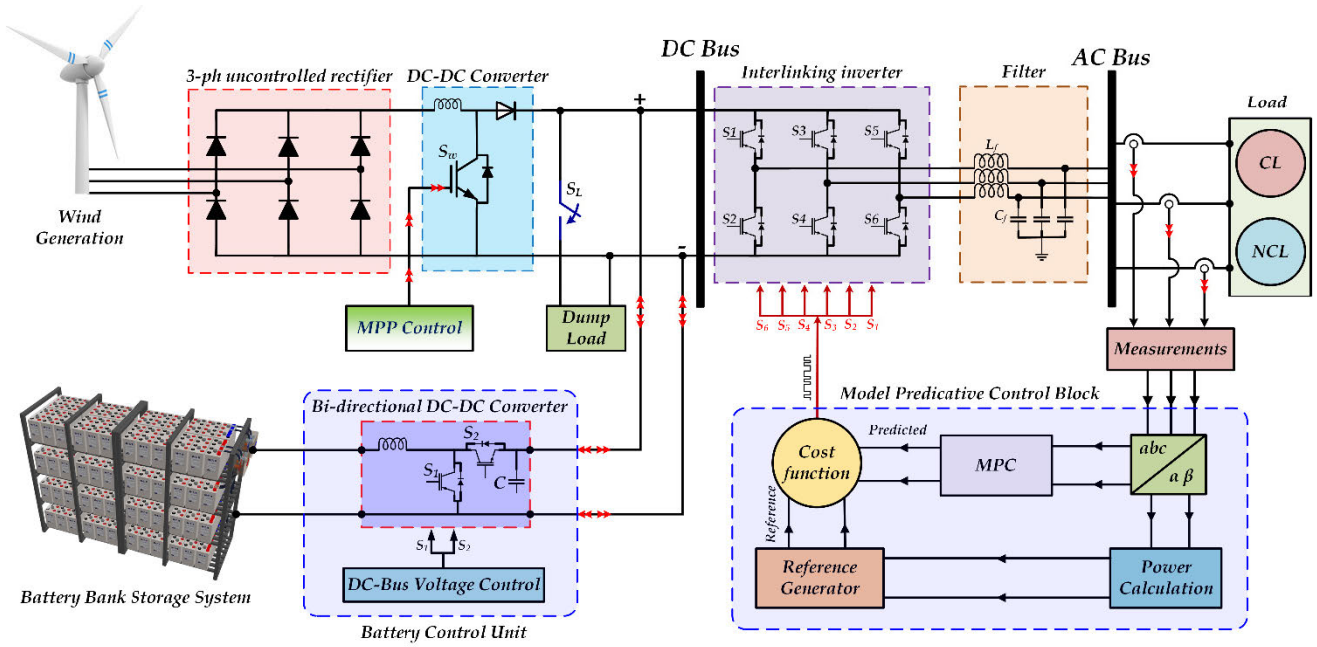

FIGURE 9. The proposed topology of PMS for HRES for residential electrification.

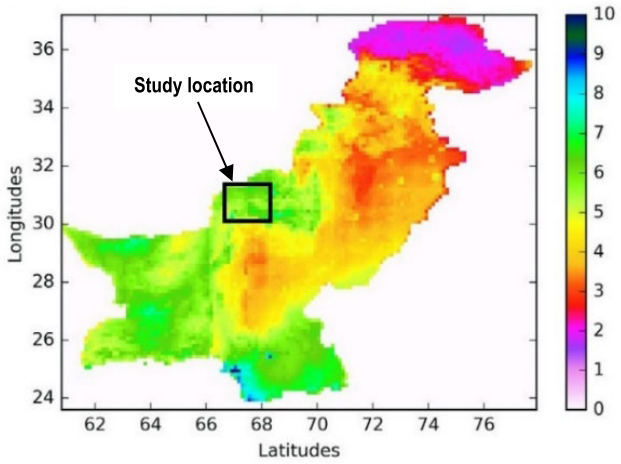

FIGURE 10. Geographical wind power atlas at 80 m height [ ].

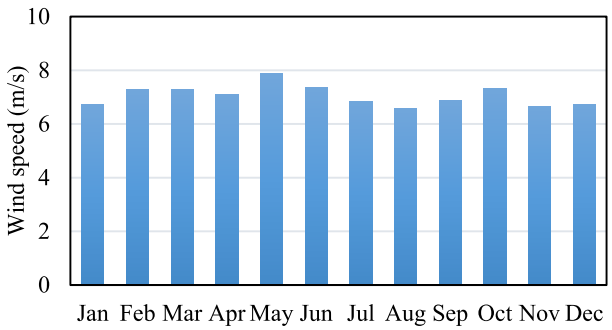

FIGURE 11. Monthly average wind speed.

where m and n are droop coefficients, V and ω are voltage and frequency for i^{th} unit.

E. POWER MANAGEMENT WITH BATTERY SOC

The battery is controlled from discharging beyond 20% of SOC and overcharging beyond 80% of SOC. Total net power is calculated based on the sum of powers from wind, diesel, and load. The load is categorized into critical (CL), non-critical (NCL) and dump (DL). DL is categorized as a load for heating purpose. Battery SOC is controlled based on upper and lower SOC limits and management strategy is shown in Figure 8. Figure 9 shows the Simulink diagram of proposed feasible wind-battery based hybrid renewable energy plan. Different case studies are discussed as follows:

VI. CASE STUDY

Pakistan is rich in wind generation capacity with potential areas in Punjab (four sites), Sindh (20 sites), Baluchistan (23 sites), Khyber Pakhtunkhwa (25 sites), FATA (two sites), Azad Jammu & Kashmir (three sites), and Gilgit Baltistan (11 sites) [53]. In Pakistan, over 51 million population is still living with a standalone microgrid, and peoples are willing to pay high electricity price for high-quality lighting, fan, and communal load [54]. Due to oil import in Pakistan, supply and demand mismatch is rapidly increasing [11]. Bright future of RE penetration in Pakistan is expected with cumulative installed wind capacity of 308MW while projects of 1140MW wind are under progress [11].

The proposed methodology for HRES design and control strategy was applied for electrification of a typical rural residential load located in Quetta city of Baluchistan Pakistan (see Fig.10) where the utility grid is not available. In Baluchistan province, wind speed range is 4-9m/s (at 10 m height) and 12.5m/s (at 50m hub height) [11].

TABLE 2. Techno-economic optimized results of feasible configurations for Quetta.

Sc.	HRES configuration	Component size			Costs				RF (%)	Fuel (L/yr)
		WT (Qty.)	DG (kW)	Converter (kW)	Initial ($)	O&M ($/yr)	NPC ($)	COE ($/kWh)		
1	WT/Battery/Converter	1	-	2.14	12,300	217.79	14,846	0.309	100	0
2	WT/DG/Battery/Converter	1	2.4	1.94	15,548	253.71	15,514	0.323	96.2	67.9
3	WT/DG/Converter	2	2.4	0.986	18,597	2,329	45,818	0.954	40.1	1,100
4	DG/Battery/Converter	-	2.4	0.539	3,036	3,989	49,661	1.030	0	1,912
5	DG (base case)	-	2.4	-	2,400	5,249	63,748	1.330	0	2,546

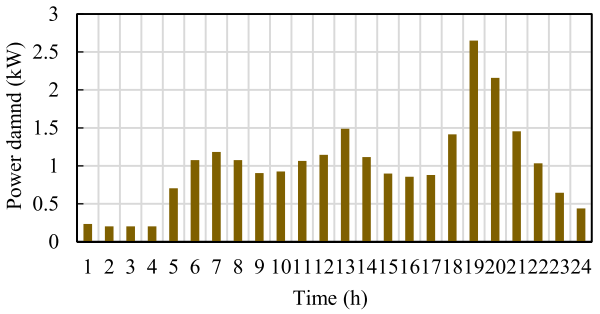

FIGURE 12. Daily load profile.

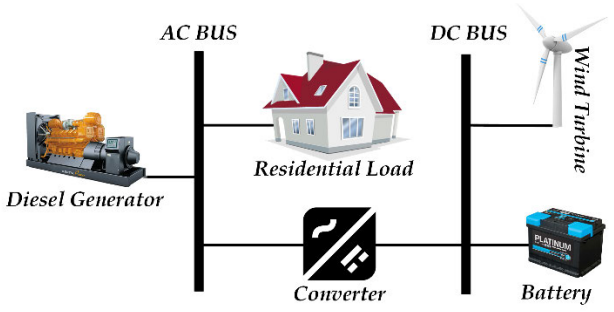

FIGURE 13. HOMER Model of the developed HRES for Quetta.

Latitude and longitude for specified location are 30°9′44″N and 66°48′68″E respectively as shown in Fig 10. Pakistan has abundant potential for the wind power generation due to its favorable climate conditions [12]. Wind speed for the selected study area was obtained from the NASA renewable energy resource website (Surface Meteorology and Solar Energy) [27]. Monthly average wind speed is shown in Figure 11 with average speed of 7 m/s. In this study, the typical electrical load of one household in Quetta city was estimated based on a local load survey. The most important energy consumption activities include lighting, TV, fans, and refrigeration. In this regard, the given load power was 2.11kW (peak value) and the annual average energy consumption was 11.25kWh/day. Fig. 12 shows the load profile of one household in the investigated area.

VII. SIMULATION RESULTS AND DISCUSSIONS

A. OPTIMAL DESIGN OF HRES

Based on the acquired data of load profile and wind speed, together with the economic and technical specifications of each component, wind, diesel, battery and converter based HRES shown in Fig.13 was modeled and simulated based on the following assumptions and constraints:

- Project lifetime was assumed 20 years as a typical value to achieve maximum extrapolation of the HRES.
- The nominal discount rate was supposed 10% according to Trading Economics for Pakistan with an expected inflation rate of 4%.
- The system was simulated considering zero capacity shortage to ensure maximum reliability.
- The operating reserve as a percentage of the load was supposed 10% to cover the sudden increase and load spikes, while the reserve power of the wind turbine was chosen 15% to compensate the random variability of the wind speed.
- A value of 20$/tons was assumed as a carbon emission penalty cost, which was considered as emission constraints.
- Load following (LF) dispatch strategy was selected to control the energy flow between different subsystems. This strategy was selected initially during the design optimization stage. Under LF strategy, when a generator is needed, it produces only enough power to meet the demand. Lower-priority objectives such as charging the battery storage or serving the deferrable load (if any) are left to the RE sources. Thus, LF seems to be suitable to achieve maximum benefits from renewable and reduce the operating hours and thus fuel consumption of the diesel. Also, it prevents the battery from excessive charge/discharges actions [30].

Table 2 shows techno-economic optimized results for all the feasible configurations of the developed HRES for Quetta ranked by NPC. Following highlights were observed.

- Among all feasible configurations, the hybridization of wind-battery-converter was of superior performance to be the optimal (or winning) configuration plan of the developed HRES for supplying the investigated area with excess electricity of 2,003 kWh.
- The winning plan consisted of one WT (2.4 kW rating), 22 batteries (2.45 kWh nominal capacity), and 2.14 kW power converter.
- The optimal system not only achieves minimum values of NPC (14, 8486$) and COE (0.309$/kWh) but also

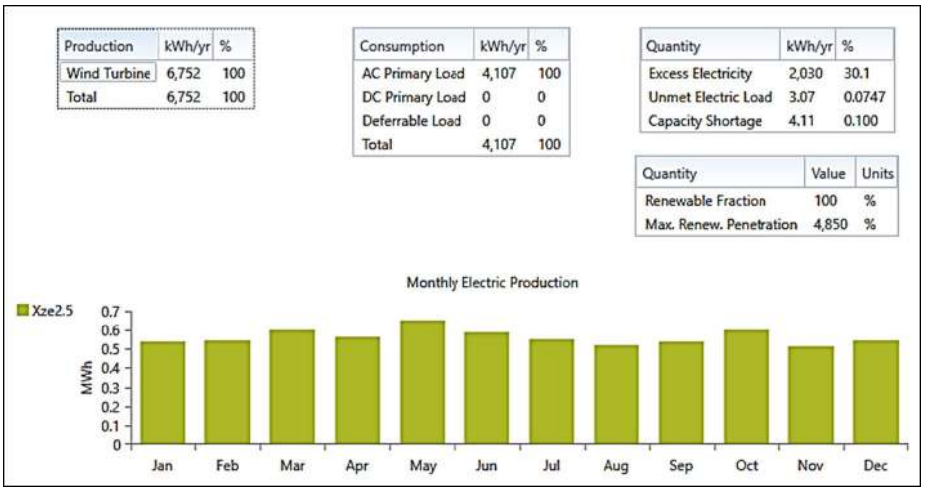

FIGURE 14. Monthly power generation profile and percentage of energy production and consumption.

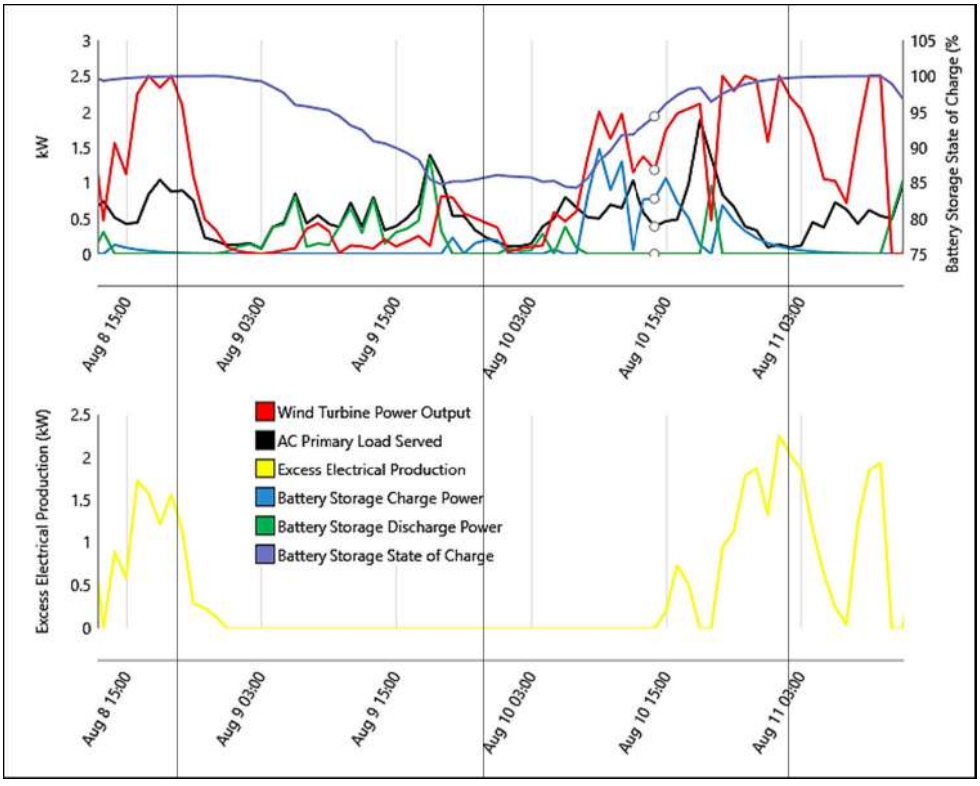

FIGURE 15. Scheduling of energy generation and consumption, sample days (August 8-11).

achieve 100% RF with zero fuel consumption and zero emission. The obtained results can give insight concerning the techno-economic and environmental viability of HRES in Pakistan.

- The worst case was the diesel-based energy system with maximum NPC and COE of 63,748$ and 1.33$/kWh caused by the expensive value of O&M cost as well as the carbon emission penalty. The annual fuel consumption of the fuel was 2,546 L/yr, while the value of the emitted CO_2 was recorded 6,664 kg/yr.

B. PERFORMANCE ASSESSMENT OF THE OPTIMAL CONFIGURATION PLAN

1) TECHNICAL ASSESSMENT

Figure 14 shows the monthly share of electricity by the wind generation system. Maximum wind power is generated and utilized to meet the load demand. Maximum wind generation is observed in May when wind speed is highest among all months (see Fig. 11).

Three days (August 8-11) are selected as a study case and is shown in Figure 15 and the real-time energy schedul-

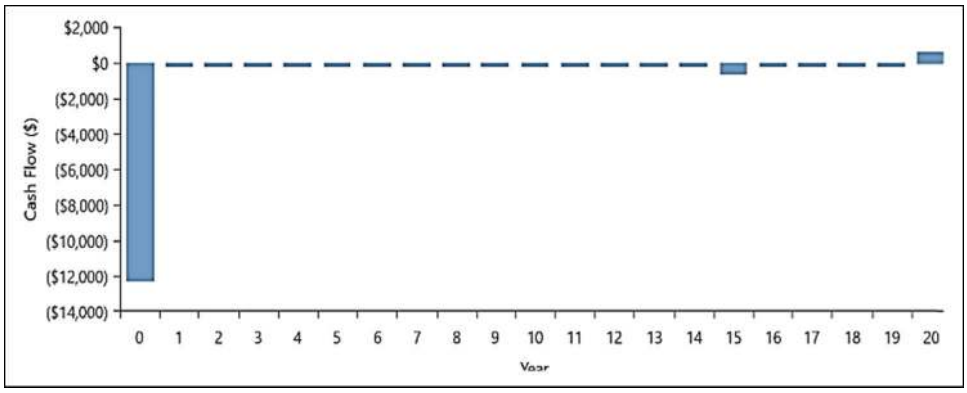

(a) Optimal case

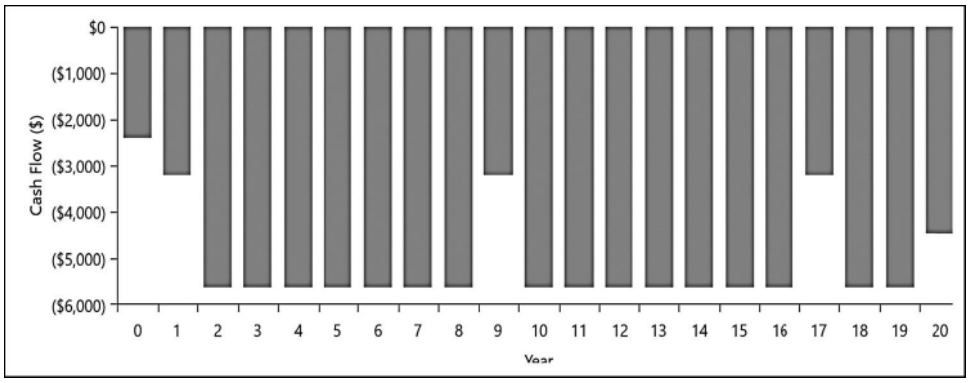

(b) Base case

FIGURE 16. Nominal cash flow results.

TABLE 3. Cost summary of the optimal configuration plan for Quetta.

Cost ($) / *Comp.*	*Capital*	*Operating*	*Replacement*	*Salvage*	*Total*
Battery Storage	3,872	2,057	0.00	187.65	5,741
Power Converter	428.2	0.00	184.63	92.99	519.9
WT	8,00	584.40	0.00	0.00	8,584
System	12,30	2,641	184.63	280.64	14,85

ing of generation and consumption is highlighted. Initially, on August 8 at 1500, AC load demand is high and wind power generation is in excess as compared to load demand. The excess energy is utilized to charge the battery. Until August 9 at 0300, load demand is continuously decreasing due to off-peak hours until morning. During this time, the battery is discharged to meet load requirement. On August 10 at 0300 onward, extra wind power is utilized to charge the battery packs and battery SOC is improved to a higher value. Highest load demand is observed at 1900 (See Figure 13). During the next day on August 11, wind power remained in excess, and extra power was utilized to charge the battery. In this way, power is managed efficiently, and 100% renewable energy penetration is ensured with minimum emission by avoiding diesel unit. Also, battery SOC remained above the lowest limit (20%) throughout the three-day simulation. Highest wind peak power is observed on August 8 after 1500,

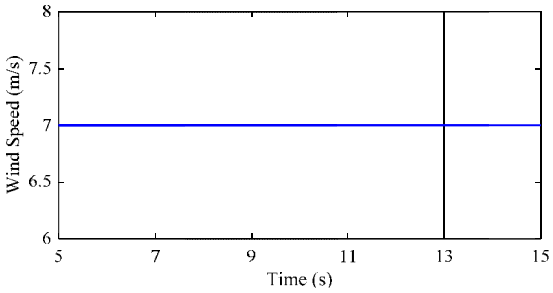

FIGURE 17. Constant wind speed of 7 m/s.

until last day when maximum wind generation can be seen to feed relatively minimum load and to charge the battery with excess energy with zero unmet loads.

2) FINANCIAL ASSESSMENT

Table 3 shows the summary of cost results for the optimal configuration plan. The initial capital cost of wind is more while battery packs have almost half capital cost as compared to wind. Operating cost of the battery storage system is more as compared to other components. Moreover, it is observed that the salvage value of the battery storage system is highest.

Fig. 16 demonstrate nominal cash flow during 20 years for base case (diesel only) and optimal case (wind-battery). Cash flow is maintained minimum constant for optimal case

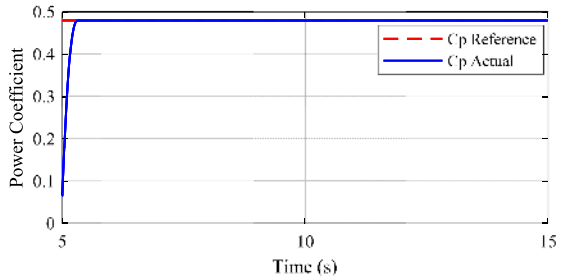

FIGURE 18. Power coefficient at a wind speed of 7 m/s.

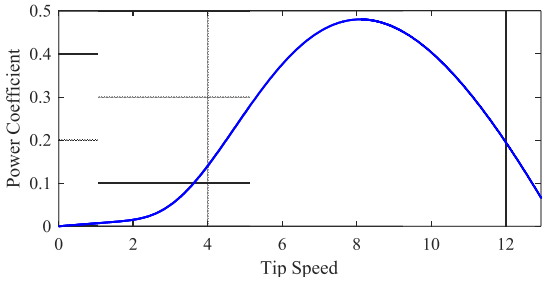

FIGURE 19. Tip speed vs. power coefficient at 7 m/s wind speed.

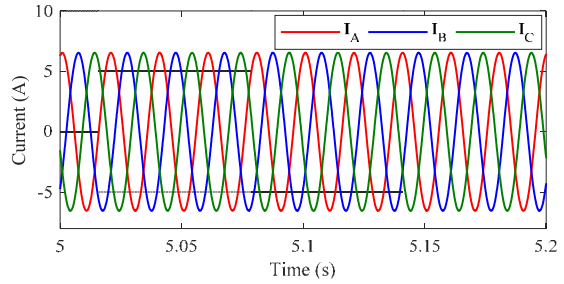

FIGURE 20. Three phase load current.

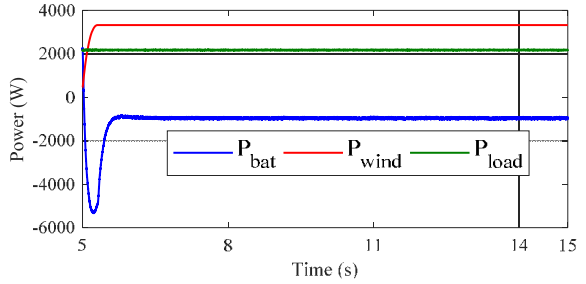

FIGURE 21. Load power-sharing between wind and battery.

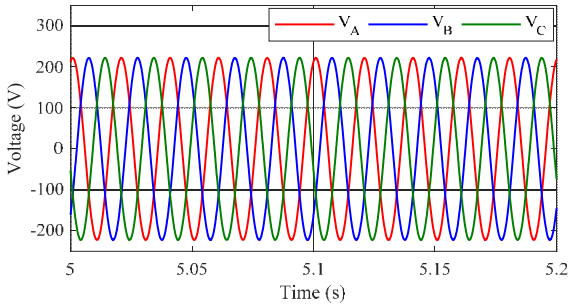

FIGURE 22. Three phase load voltage.

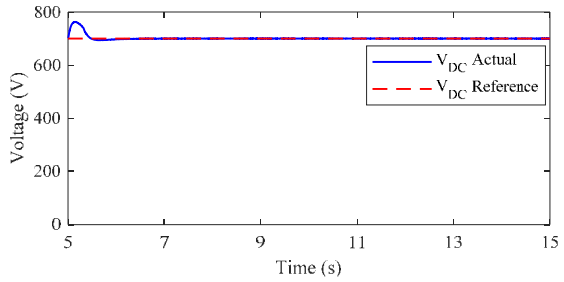

FIGURE 23. DC bus voltage using a battery controller.

throughout the project lifetime, while the value for the base case is continuously increasing and reaching the highest peak until the end of the project lifetime.

C. POWER MANAGEMENT AND CONTROL STRATEGY

A control strategy is applied by using model predictive control under different circumstances of variable load conditions and fluctuating wind speed.

1) CONSTANT LOAD WITH FIXED WIND SPEED

Constant wind speed of 7 m/s is applied, as shown in Figure 17 throughout the simulation time. While maximum wind power extraction can be analyzed from the value of power coefficient, Cp (0.48), as shown in Figure 18. Tip speed vs power coefficient is shown in Figure 19, which shows that the tip speed of 8 is the optimum value at which optimum power coefficient of 0.48 can be achieved for maximum wind power extraction.

The model predictive control strategy is applied for interlinking inverter control. Figure 20 shows three phase load currents during constant load, while power-sharing is shown in Figure 21. It can be observed that maximum wind power extraction is successfully implemented by using wind boost converter control. The constant load is served by wind power. In this case, wind power generation is greater than the load demand. Therefore, extra power is used to charge the battery, as shown in Figure 21. Pure sinusoidal waveform of three phases load voltage is obtained by MPC inverter control, as shown in Figure 22, while constant DC bus voltage is maintained through the battery controller as depicted in Figure 23.

2) CONSTANT LOAD UNDER VARIABLE WIND SPEED

Variable wind speed is applied (Figure 24) to show the effect of variable source on DC bus voltage and load power sharing. Wind speed variation from 7 m/s to 6.5 m/s is investigated. During wind speed variation, power exchange phenomenon is shown in Figure 25. It is observed that despite wind speed declination, wind power generation is reduced, but wind boost controller is still controlling maximum wind power extraction while battery-charging power is reduced due to low wind power generation and wind power unit continuously

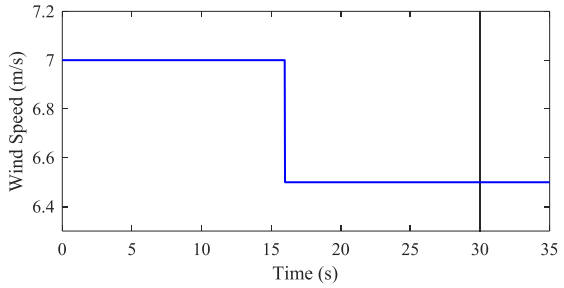

FIGURE 24. Wind speed variation from 7 m/s to 6.5 m/s.

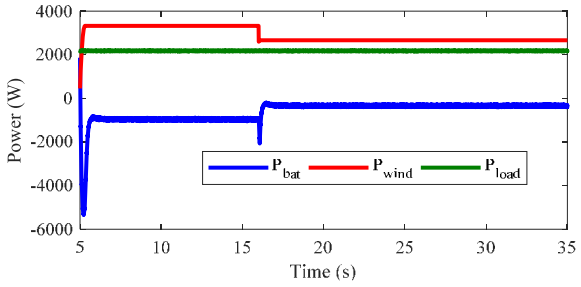

FIGURE 25. Power exchange with variable wind speed.

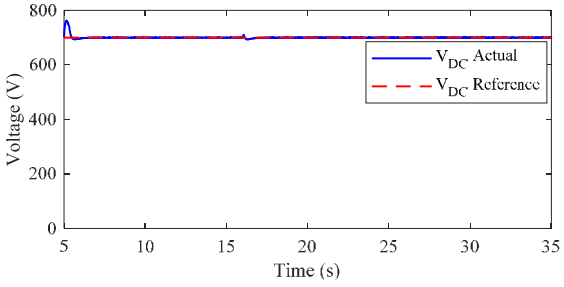

FIGURE 26. DC bus voltage at fluctuating wind speed.

meet the load demand. DC bus voltage is also maintained constant during this process, as shown in Figure 26.

3) VARIABLE LOAD WITH CONSTANT WIND SPEED

At 22 s of simulation, variable load is applied as shown in Figure 28 while applying constant wind power at 6 m/s as illustrated in Figure 27. Prior to load variation to higher level, wind power generation is more than load demand, and extra wind energy is utilized to charge the battery. During abrupt load penetration at 22 s, load demand is more than wind power generation, and excess power demand is met by discharging the battery, as shown in Figure 28. Figure 29 clearly shows that the DC bus voltage remains stable during abrupt load variations.

4) VARIABLE LOAD WITH FLUCTUATING WIND SPEED

The final case is analyzed with both external disturbances of source and load. Fluctuating wind speed, along with abrupt load changes will show a clear picture of the hybrid renewable energy system. At 16 s, wind speed is changed from 7 m/s

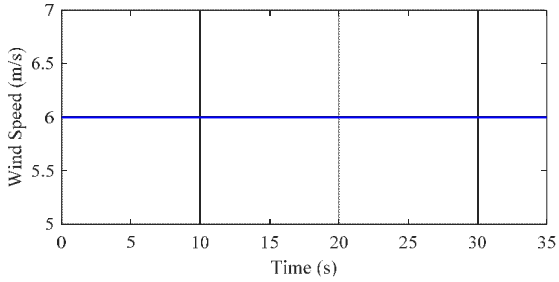

FIGURE 27. Constant wind speed of 6 m/s.

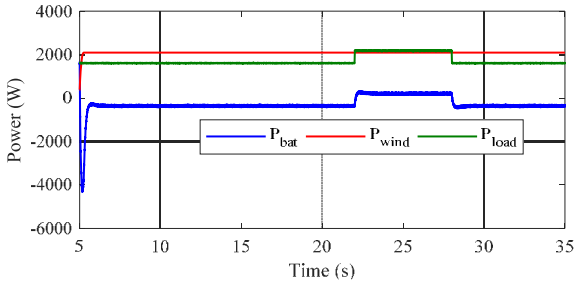

FIGURE 28. Power allocation at variable load and constant wind speed.

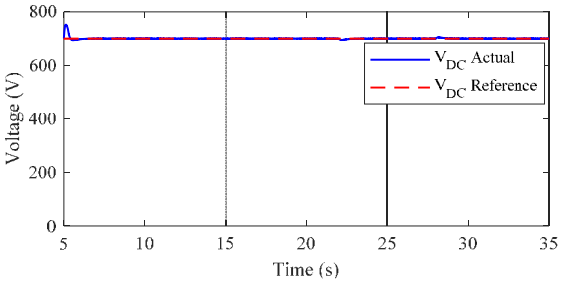

FIGURE 29. DC bus voltage during load variation and fix wind speed.

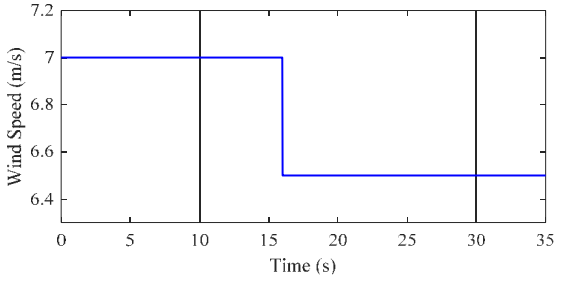

FIGURE 30. Wind speed variation from 7 m/s to 6.5 m/s.

to 6.5 m/s while power allocation is shown in Figure 31. It is clearly shown that wind power is decreased due to wind speed reduction. At 22 s, load is increased, and wind power is sufficient to fulfill extra load demand. During the whole simulation, battery is seen to handle the intermittent nature of fluctuating wind generation while load following strategy at generation side is incorporated and control strategy remained successful according to the proposed work.

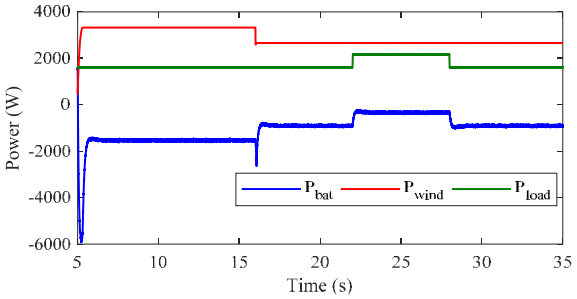

FIGURE 31. Power sharing during variable load and fluctuating wind.

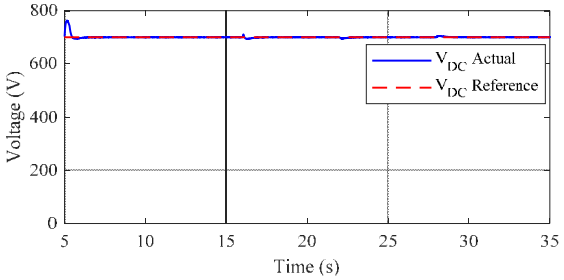

FIGURE 32. DC bus voltage during variable wind and fluctuating load.

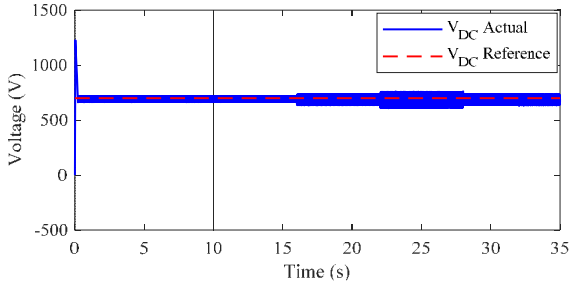

FIGURE 33. Fluctuating DC bus voltage due to variable source and load.

5) PERFORMANCE ANALYSIS OF CONVENTIONAL PI VS MPC CONTROLLER

Until now, MPC inverter control strategy is successfully implemented. To validate this MPC strategy, it is compared with the conventional PI control strategy. Fluctuating DC bus voltage is generated by abrupt variation of load and source. The PI control strategy is analyzed first. Ripples are observed in three-phase load voltage, as shown in Figure 34 and Figure 35, while load current is shown in Figure 36 and Figure 37. Pure sinusoidal waveforms without any ripples are observed during MPC implementation, as shown in Figure 38 and Figure 39 for load voltages. Figure 40 and Figure 41 shows a three-phase load current when the MPC method is employed. It is observed from Figure 42 and Figure 43 that total harmonic distortion (THD) for PI control scheme is more (2.05%) as compared to MPC scheme where 0.24% THD is found. These results and discussion clearly show the successful and promising results incorporated during MPC methodology.

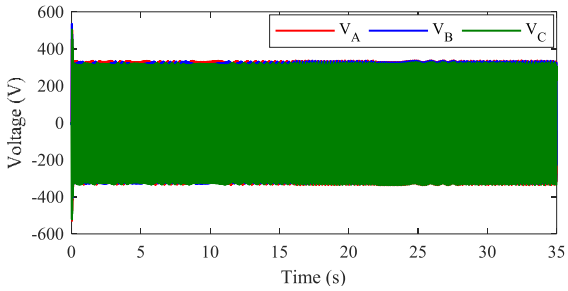

FIGURE 34. Three phase load voltage during DC bus voltage variation (PI control).

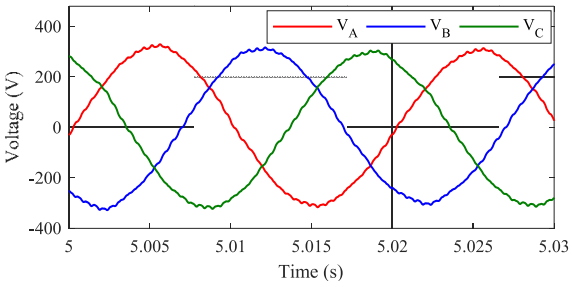

FIGURE 35. Zoomed load voltage during variable DC voltage (PI control).

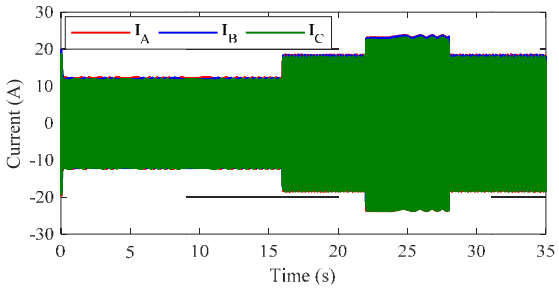

FIGURE 36. Load current with source and load disturbances (PI control).

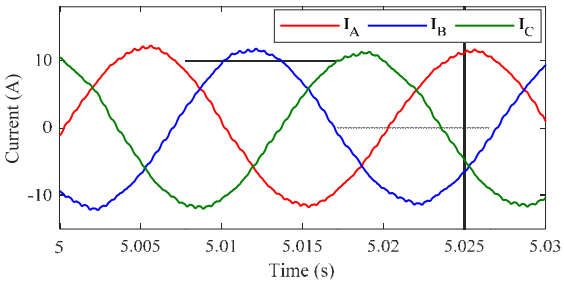

FIGURE 37. Zoomed load current (PI control).

6) BATTERY SOC MANAGEMENT

To effectively control battery SOC and maximum utilization of wind energy, power management strategy depicted in Fig. 8 is implemented. At 22 s, wind speed is reduced from 6.4 m/s and 6.2 m/s as shown in Figure 44. DC bus voltage,

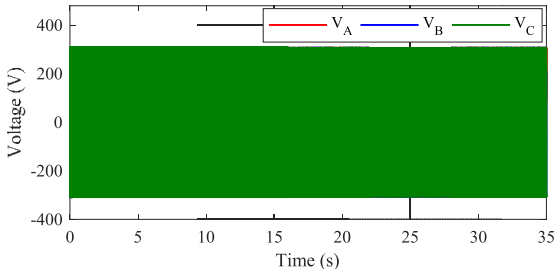

FIGURE 38. Load voltage (MPC control).

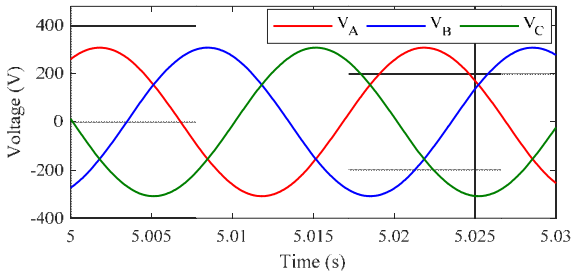

FIGURE 39. Zoomed three phase load voltage (MPC control).

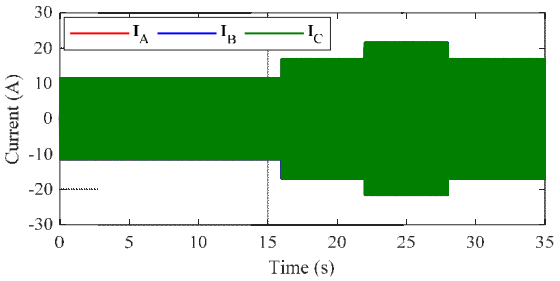

FIGURE 40. Load current (MPC control).

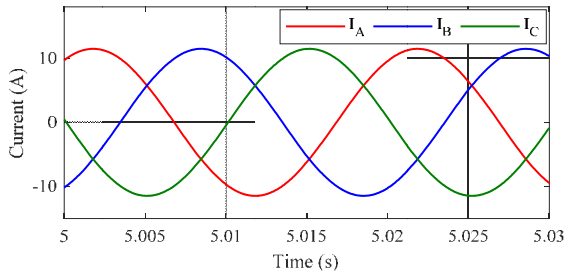

FIGURE 41. Zoomed three phase load current (MPC control).

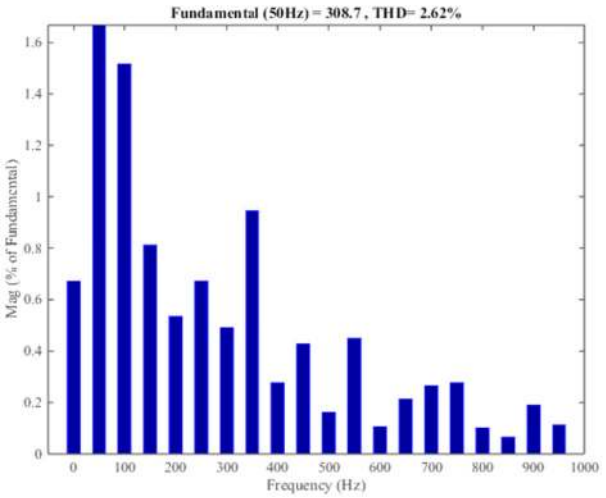

FIGURE 42. Total harmonic distortion (THD) during PI control.

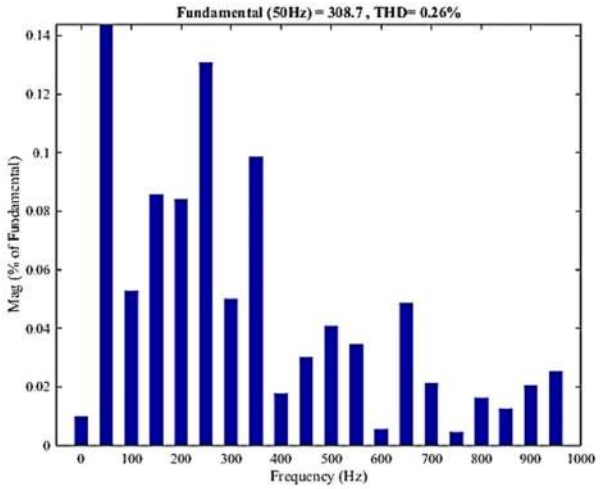

FIGURE 43. Total harmonic distortion (THD) during MPC control.

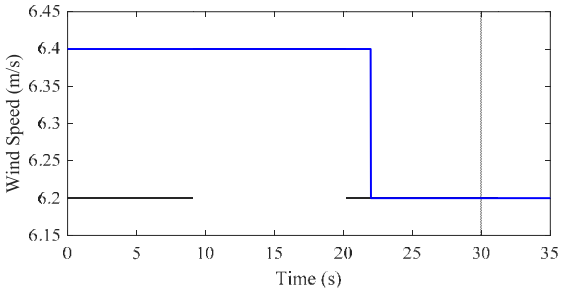

FIGURE 44. Wind speed variation from 6.4 m/s to 6.2 m/s.

RMS load voltage, and load current are shown in Figure 45, Figure 46, and Figure 47, respectively.

After injecting wind at 8s, wind power is feeding the load the battery is charged as shown in Figure 48 and Figure 49 respectively. As the battery SOC is reached the maximum limit of 80% at 12.5 s (see Figure 51), the management strategy is activated and switching command signal is sent to feed extra power of wind and battery to non-critical load (NCL). In this way, battery SOC will be controlled to avoid maximum limit while feeding dump heating load for auxiliary applications in case of surplus energy. At 22 s, when wind power is reduced (see Figure 48), battery is further discharged as shown in Figure 49 to maintain load demand (see Figure 50). Fig. 51 shows battery SOC, which is continuously discharging until it will reach a minimum SOC level of 20%. In this way, battery SOC will remain within the limit and battery cost will be minimized.

TABLE 4. Comparison between design optimization results of proposed HRES and literature.

REF	Region	HRES Plan	NPC ($)	COE ($/kWh)
[5]	Canada	PV/Wind/Biomass (/Natural gas)/Battery/Converter	29300000	0.285
[4]	India	Wind/PV/Battery/Converter	228353	0.288
[9]	Nigeria	Diesel generator/PV/Wind/Battery/Converter	10733	0.459
[16]	India	PV/Biomass gasifier/Diesel /Battery/Converter	123668	0.145
[40]	South Africa	PV/Wind /Fuel cell/Converter	38400000	7.540
[32]	Egypt	PV/Wind /Diesel/battery/Converter	1684118	0.190
[55]	Benin	PV /Diesel/ battery/Converter	555492	0.207
[39]	Iraq	PV/Hydro/Diesel/Battery/Converter	113201	0.054
[56]	Ethiopia	PV/Wind /Diesel/battery/Converter	82734	0.207
[23]	Algeria	PV /Diesel/ battery/Converter	8585.14	0.380
Current study	Pakistan	WT /DG/ battery/Converter	14846	0.309

TABLE 5. Comparison of proposed PMS strategy vs published ones.

Ref	Sizing Optimization (Outer loop)	SOC based EMS (Inner loop)	PI based EMS	MPC based EMS	MPC based load voltage/frequency control
[30]	Yes	Yes	No	No	No
[47]	No	Yes	Yes	No	No
[48]	No	Yes	Yes	Yes	Yes
[32]	Yes	No	No	No	No
[51]	No	No	No	No	Yes
[63]	No	No	No	No	Yes
[58]	No	No	No	No	Yes
[64]	No	No	No	No	Yes
[65]	No	No	No	No	Yes
[59]	No	No	No	No	Yes
[66]	No	No	No	No	Yes
[60]	No	No	No	No	Yes
[61]	No	No	No	No	Yes
[67]	No	No	No	No	Yes
[68]	No	No	No	No	Yes
[62]	No	No	No	No	Yes
[69]	No	No	No	No	Yes
[70]	No	No	No	No	No
Proposed	Yes	Yes	Yes	Yes	Yes

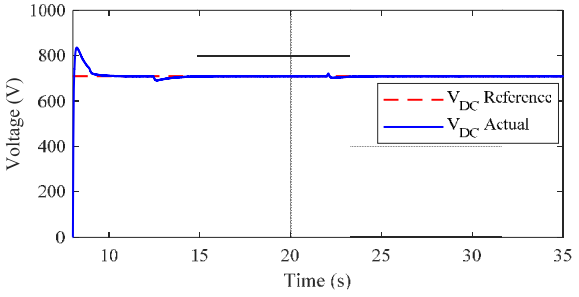

FIGURE 45. DC bus voltage during wind speed variation.

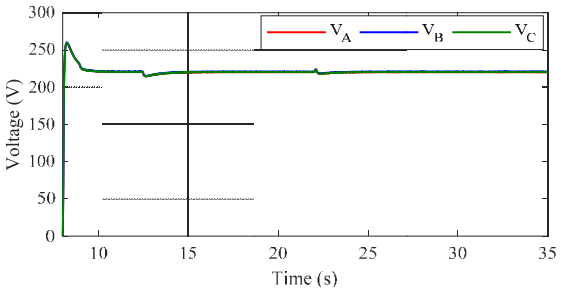

FIGURE 46. RMS load voltage during wind speed variation.

VIII. COMPARISON BETWEEN PROPOSED SYSTEM FEATURES WITH RESULTS AND LITERATURE

First, in terms of design optimization results of HRES, Table 4 shows comparison between cost results of the proposed HRES in Pakistan and those results of different hybrid systems plans implemented in different countries. Because of the value of NPC was calculated based on equipment sizes and local initial investments, its value was implicitly unequal for the presented HRESs. Nevertheless, the value of COE can be used as an alternative and as a valued metric of the cost of renewable energy generation. From the given table, it is seen that Iraq and India had the lowest COE when compared to other countries. On the other hand, the COE in South Africa was the higher. Regarding the obtained results by this study,

TABLE 6. Comparison of proposed PMS strategy vs published ones.

Ref	Wind MPPT control (Boost)	Wind Rectifier	DC voltage controller (buck-boost)	Inverter Control (PI)	Inverter Control (MPC)	THD Analysis
[30]	No	No	No	No	No	No
[19]	No	No	No	No	No	No
[47]	Yes	No	Yes	No	No	No
[48]	No	No	Yes	No	Yes	No
[32]	No	No	No	No	No	No
[51]	No	No	No	Yes	Yes	Yes
[63]	No	Controlled	No	Yes	Yes	No
[58]	No	No	No	Yes	Yes	Yes
[64]	No	Controlled	No	No	No	No
[65]	No	No	No	No	Yes	Yes
[59]	No	No	No	No	Yes	Yes
[66]	No	No	No	No	Yes	No
[60]	No	No	Yes	Yes	Yes	Yes
[61]	No	Controlled	No	Yes	Yes	Yes
[67]	No	Controlled	No	No	Yes	No
[68]	No	No	No	Yes	Yes	No
[62]	No	No	MPC	No	Yes	Yes
[69]	No	Controlled	No	No	No	No
[70]	No	No	No	Yes	No	No
Proposed	Yes	Uncontrolled	Yes	Yes	Yes	Yes

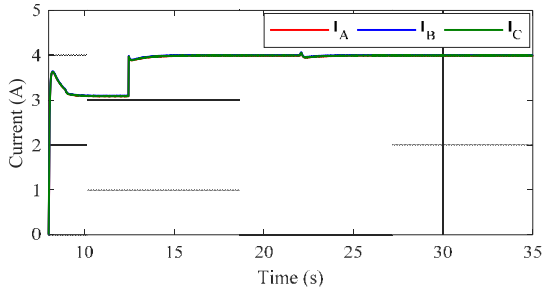

FIGURE 47. RMS load current.

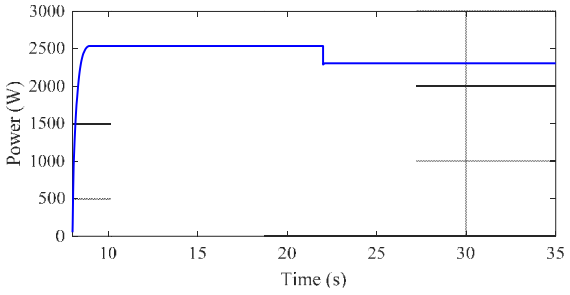

FIGURE 48. Maximum wind power generation during variable speed.

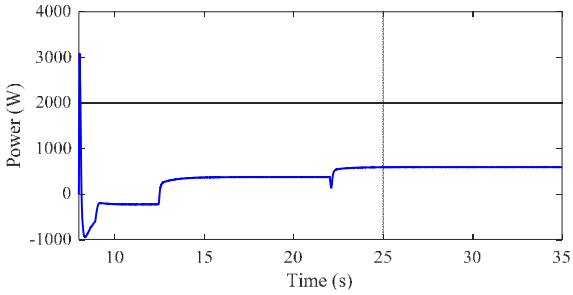

FIGURE 49. Battery power.

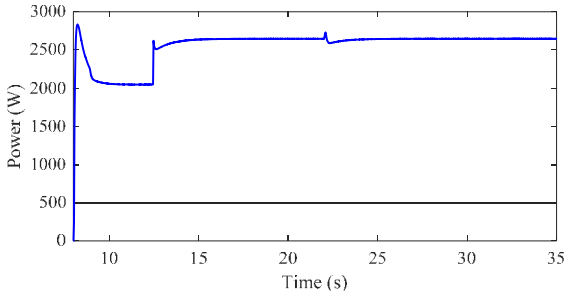

FIGURE 50. Load power.

the comparison also shows a good agreement with the other works and can give insight regarding the financial feasibility of HRES in Pakistan.

Second, in terms of the performance evaluation of the developed PMS of HRES, Table 5 shows comparison of energy management and control between the proposed approach and the published literature. Results show that most of the published work implemented MPC based load control but it was not thoroughly investigated on the basis of optimal sizing, SOC management and EMS comparison between PI and MPC. Table 6 compares the analysis of different controllers between current study and the literature. As compared to controlled rectifier, the proposed model with uncontrolled rectifier is simple, and low cost. Further, No IGBTs, and additional controller with control signals are required which reduces the model complexity as well as the system cost. Results show that mostly published work was not analyzed with the consideration of wind MPPT, uncontrolled rectifier, DC-DC battery controller, THD analysis, PI and MPC based inverter control. Table 7 shows the comparison of total harmonic distortion (THD) between PI and MPC for the proposed strategy and the literature. Results show that

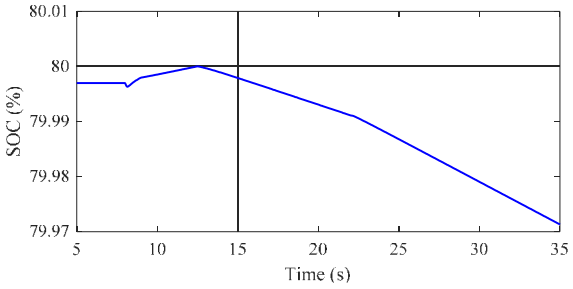

FIGURE 51. Battery SOC.

TABLE 7. Performance comparison of the proposed MPC against PI.

Ref	THD (%)	
	PI	MPC
[51]	7.10	3.69
[57]	5.35	4.65
[58]	-	2.8
[59]	-	>0.5
[60]	-	3.93
[61]	7.47	13.53
[62]	-	3.69
Current study	2.62	0.26

TABLE 8. Performance comparison of the proposed PMS against PI.

Proposed	THD (%)	DC Voltage Ripples	Load Power Ripples
PI	2.62	±50V (5s-16s)	±1000W (5s-8s)
		±55V (16s-22s)	±1200W (8s-11s)
		±95V (22s-28s)	±1000W (11s-15s)
		±55V (28s-35s)	
PMS	0.26	±1.3V (5s-16s)	±20W (5s-8s)
		±0.8V (16s-22s)	±30W (8s-11s)
		±1V (22s-28s)	±20W (11s-15s)
		±1V (28s-35s)	

the minimum value of THD i.e. 2.62% is obtained for PI control in the proposed study as compared to higher THD values. Similarly, 0.26% THD for MPC approach is obtained which the minimum value among all THD's mentioned in the literature.

Also, Table 8 shows the comparison between MPC and PI for the current study with %THD, magnitude variations of DC voltage and load power ripples during load fluctuations. Results show that the maximum DC voltage deviation of 95V is observed during 22-28s for PI control while maximum deviation of only 1.3V at 5-16s is observed for the proposed PMS approach. Further, the deviation of power ripples is drastically reduced from the maximum value of 1200W (for PI) into 30W (for MPC) at 8-11s.

IX. CONCLUSION

This paper established a feasible and economically viable model of WT/DG/battery/converter hybrid energy for domestic load in Pakistan by handling intermittent nature of RE resources, and abrupt load variations. Based on techno-economic and simulation results conducted with the aid of HOMER software, optimal component sizing of HRES is achieved, and the most feasible configuration plan based on WT, battery and converter has been proposed. Advance and adequate PMS has also been applied for the winning plan using model predictive control with the help of MATLAB/Simulink.

The simulation results have validated the proposed management and control scheme and are verified under different conditions of variable loads and fluctuating wind speed. Practical load profile data and real weather data are taken to investigate simulation studies.

Main highlights of the current work are as follows:

- The optimal configuration plan with (WT/DG/battery/converter) is obtained with the least NPC and COE of 14,846$ and 0.309$/kWh, respectively. So, 100% penetration of RESs is guaranteed, together with zero electricity shortage
- COE is more when diesel is included (case-2). Therefore, the critical role of diesel generator with carbon emission penalty is observed for standalone domestic HRES.
- NPC of the proposed model is about four times less ($14846) than base case ($63748). Therefore, diesel only is not recommended during standalone operation, which is a normal tradition in Pakistan during standalone operation.
- Carbon emission and fuel consumption for the proposed system are zero. Total fuel consumption is 2546L/yr for the base case while it is zero for the optimal case.
- The applied PMS is verified with promising results under different conditions of variable loads and fluctuating wind speed.
- FCS-MPC based primary control is applied for an isolated HRES with improved output power quality.
- Proposed MPC based strategy takes less rise and fall time as compared to the conventional PI control scheme under fluctuating DC bus voltage.
- Proposed methodology improves voltage error and fully tracking the reference voltage with zero steady-state error and stable microgrid operation.
- THD of 0.26% for the load voltage is obtained.
- By regulating voltage magnitude, the proposed scheme ensures better power quality under steady state and transient response of the system.
- Power management with battery SOC is also explained under the variable power supply and abrupt load changes.
- Optimal PI controllers are used to extract the maximum wind power and regulation of DC bus voltage.

With great potential for improvement in smart grid systems, the developed model of this paper will help governments and planners to implement attractive policies and mechanism by encouraging fast integration of more RERs to the existing energy systems to provide reliable, cost-effective and eco-friendly hybrid energy infrastructure. Future work is to include different load patterns along with additional energy

sources (PV, hydro, FC, and biomass) and sensitivity analysis to investigate the multidimensional impacts of uncertain parameters on the system design and management.

APPENDIX

The parameters of battery inductance design are as follows [34]:

$$\Delta I_{bat} = 20\% I_{bat}, \quad I_{bat} < I_{bat(max)}, \quad D_{Bat} = V_{DC}/V_{Bat}$$

ACKNOWLEDGMENT

The authors would like to thank the State Key Laboratory of Advanced Electromagnetic Engineering and Technology, Huazhong University of Science and Technology to provide research environment for successful implementation of the proposed strategy.

REFERENCES

[1] A. L. Bukar and C. W. Tan, "A review on stand-alone photovoltaic-wind energy system with fuel cell: System optimization and energy management strategy," *J. Clean. Prod.*, vol. 221, pp. 73–88, Jun. 2019.
[2] Y. Sawle, S. C. Gupta, and A. K. Bohre, "Socio-techno-economic design of hybrid renewable energy system using optimization techniques," *Renew. Energy*, vol. 119, pp. 459–472, Apr. 2018.
[3] L. Bartolucci, S. Cordiner, V. Mulone, and J. L. Rossi, "Hybrid renewable energy systems for household ancillary services," *Int. J. Elect. Power Energy Syst.*, vol. 107, pp. 282–297, May 2019.
[4] O. Krishan and S. Suhag, "Techno-economic analysis of a hybrid renewable energy system for an energy poor rural community," *J. Energy Storage*, vol. 23, pp. 305–319, Jun. 2019.
[5] M. Bagheri, S. H. Delbari, M. Pakzadmanesh, and C. A. Kennedy, "City-integrated renewable energy design for low-carbon and climate-resilient communities," *Appl. Energy*, vol. 239, pp. 1212–1225, Apr. 2019.
[6] S. Bahramara, M. P. Moghaddam, and M. R. Haghifam, "Optimal planning of hybrid renewable energy systems using HOMER: A review," *Renew. Sustain. Energy Rev.*, vol. 62, pp. 609–620, Sep. 2016.
[7] F. K. Abo-Elyousr and A. Elnozahy, "Bi-objective economic feasibility of hybrid micro-grid systems with multiple fuel options for islanded areas in Egypt," *Renew. Energy*, vol. 128, pp. 37–56, Dec. 2018.
[8] M. Elkadeem, S. Wang, E. Atia, M. Shafik, S. W. Sharshir, Z. Ullah, and H. Chen, "Techno-economic design and assessment of grid-isolated hybrid renewable energy system for agriculture sector," in *Proc. 14th IEEE Conf. Ind. Electron. Appl. (ICIEA)*, Jun. 2019.
[9] E. O. Diemuodeke, A. Addo, C. O. C. Oko, Y. Mulugetta, and M. M. Ojapah, "Optimal mapping of hybrid renewable energy systems for locations using multi-criteria decision-making algorithm," *Renew. Energy*, vol. 134, pp. 461–477, Apr. 2019.
[10] *Global Trend in Wind Energy Investment*. Accessed: May 10, 2019. [Online]. Available: http//www.fs-unep-centre.org
[11] M. Kamran, "Current status and future success of renewable energy in Pakistan," *Renew. Sustain. Energy Rev.*, vol. 82, pp. 609–617, Feb. 2018.
[12] A. Ashfaq and A. Ianakiev, "Features of fully integrated renewable energy atlas for Pakistan; wind, solar and cooling," *Renew. Sustain. Energy Rev.*, vol. 97, pp. 14–27, Dec. 2018.
[13] C. Bastholm and F. Fiedler, "Techno-economic study of the impact of blackouts on the viability of connecting an off-grid PV-diesel hybrid system in Tanzania to the national power grid," *Energy Convers. Manag.*, vol. 171, pp. 647–658, Sep. 2018.
[14] A. Kaabeche, M. Belhamel, and R. Ibtiouen, "Sizing optimization of grid-independent hybrid photovoltaic/wind power generation system," *Energy*, vol. 36, no. 2, pp. 1214–1222, 2011.
[15] A. Roth, M. Boix, V. Gerbaud, L. Montastruc, and P. Etur, "A flexible metamodel architecture for optimal design of Hybrid Renewable Energy Systems (HRES)—Case study of a stand-alone HRES for a factory in tropical island," *J. Clean. Prod.*, vol. 223, pp. 214–225, Jun. 2019.
[16] R. Rajbongshi, D. Borgohain, and S. Mahapatra, "Optimization of PV-biomass-diesel and grid base hybrid energy systems for rural electrification by using HOMER," *Energy*, vol. 126, pp. 461–474, May 2017.
[17] L. Li, Z. Yao, S. You, C.-H. Wang, C. Chong, and X. Wang, "Optimal design of negative emission hybrid renewable energy systems with biochar production," *Appl. Energy*, vol. 243, pp. 233–249, Apr. 2019.
[18] M. R. Akhtari and M. Baneshi, "Techno-economic assessment and optimization of a hybrid renewable co-supply of electricity, heat and hydrogen system to enhance performance by recovering excess electricity for a large energy consumer," *Energy Convers. Manag.*, vol. 188, pp. 131–141, May 2019.
[19] P. Rullo, L. Braccia, P. Luppi, D. Zumoffen, and D. Feroldi, "Integration of sizing and energy management based on economic predictive control for standalone hybrid renewable energy systems," *Renew. Energy*, vol. 140, pp. 436–451, Sep. 2019.
[20] T. Ma and M. S. Javed, "Integrated sizing of hybrid PV-wind-battery system for remote island considering the saturation of each renewable energy resource," *Energy Convers. Manag.*, vol. 182, pp. 178–190, Feb. 2019.
[21] T. Ma and M. S. Javed, "Techno-economic assessment of a hybrid solar-wind-battery system with genetic algorithm," in *Proc. 10th Int. Conf. Appl. Energy*, vol. 176, 2018, pp. 704–717.
[22] H. Rezk, E. T. Sayed, M. Al-Dhaifallah, M. Obaid, A. H. M. El-Sayed, M. A. Abdelkareem, and A. G. Olabi, "Fuel cell as an effective energy storage in reverse osmosis desalination plant powered by photovoltaic system," *Energy*, vol. 175, pp. 423–433, May 2019.
[23] F. Fodhil, A. Hamidat, and O. Nadjemi, "Potential, optimization and sensitivity analysis of photovoltaic-diesel-battery hybrid energy system for rural electrification in Algeria," *Energy*, vol. 169, pp. 613–624, Feb. 2019.
[24] A. Tajeddin and E. Roohi, "Designing a reliable wind farm through hybridization with biomass energy," *Appl. Therm. Eng.*, vol. 154, pp. 171–179, May 2019.
[25] A. B. Forough and R. Roshandel, "Lifetime optimization framework for a hybrid renewable energy system based on receding horizon optimization," *Energy*, vol. 150, pp. 617–630, May 2018.
[26] A. K. Nag and S. Sarkar, "Modeling of hybrid energy system for futuristic energy demand of an Indian rural area and their optimal and sensitivity analysis," *Renew. Energy*, vol. 118, pp. 477–488, Apr. 2018.
[27] *Wind System Installation*. Accessed: May 10, 2019. [Online]. Available: https://www.windenergy.com
[28] A. C. Duman and Ö. Güler, "Techno-economic analysis of off-grid PV/wind/fuel cell hybrid system combinations with a comparison of regularly and seasonally occupied households," *Sustain. Cities Soc.*, vol. 42, pp. 107–126, Oct. 2018.
[29] X. Gai, Y. Wang, R. Chen, and L. Zou, "Research on hybrid microgrid based on simultaneous AC and DC distribution network and its power router," *Energies*, vol. 12, no. 6, p. 1077, 2019.
[30] A. S. Aziz, M. F. N. Tajuddin, M. R. Adzman, M. A. M. Ramli, and S. Mekhilef, "Energy management and optimization of a PV/diesel/battery hybrid energy system using a combined dispatch strategy," *Sustainability*, vol. 11, no. 3, p. 683, 2019.
[31] *HOMER Software Optimization Tool*. Accessed: May 6, 2019. [Online]. Available: https://www.homerenergy.com
[32] F. Diab, H. Lan, L. Zhang, and S. Ali, "An environmentally friendly factory in Egypt based on hybrid photovoltaic/wind/diesel/battery system," *J. Clean. Prod.*, vol. 112, pp. 3884–3894, Jan. 2016.
[33] K. Murugaperumal and P. A. D. V. Ajay, "Energy storage based MG connected system for optimal management of energy: An ANFMDA technique," *Int. J. Hydrogen Energy*, vol. 44, no. 16, pp. 7996–8010, 2019.
[34] J. Abushnaf and A. Rassau, "Impact of energy management system on the sizing of a grid-connected PV/Battery system," *Electr. J.*, vol. 31, no. 2, pp. 58–66, 2018.
[35] A. González, J. R. Riba, and A. Rius, "Optimal sizing of a hybrid grid-connected photovoltaic–wind–biomass power system," *Sustainability*, vol. 7, no. 9, pp. 12787–12806, 2015.
[36] M. Jahangiri, A. Haghani, A. A. Shamsabadi, A. Mostafaeipour, and L. M. Pomares, "Feasibility study on the provision of electricity and hydrogen for domestic purposes in the south of Iran using grid-connected renewable energy plants," *Energy Strateg. Rev.*, vol. 23, pp. 23–32, Jan. 2019.
[37] M. A. H. Mondal and A. K. M. S. Islam, "Potential and viability of grid-connected solar PV system in Bangladesh," *Renew. Energy*, vol. 36, no. 6, pp. 1869–1874, 2011.
[38] M. A. Omar and M. M. Mahmoud, "Grid connected PV-home systems in Palestine: A review on technical performance, effects and economic feasibility," *Renew. Sustain. Energy Rev.*, vol. 82, pp. 2490–2497, Feb. 2018.

[39] A. S. Aziz, M. F. N. Tajuddin, M. R. Adzman, A. Azmi, and M. A. M. Ramli, "Optimization and sensitivity analysis of standalone hybrid energy systems for rural electrification: A case study of Iraq," *Renew. Energy*, vol. 138, pp. 775–792, Aug. 2019.

[40] D. N. Luta and A. K. Raji, "Decision-making between a grid extension and a rural renewable off-grid system with hydrogen generation," *Int. J. Hydrogen Energy*, vol. 43, no. 20, pp. 9535–9548, 2018.

[41] H. Ren, Q. Wu, W. Gao, and W. Zhou, "Optimal operation of a grid-connected hybrid PV/fuel cell/battery energy system for residential applications," *Energy*, vol. 113, pp. 702–712, Oct. 2016.

[42] C. Y. Acevedo-Arenas, A. Correcher, C. Sánchez-Díaz, E. Ariza, D. Alfonso-Solar, C. Vargas-Salgado, and J. F. Petit-Suárez, "MPC for optimal dispatch of an AC-linked hybrid PV/wind/biomass/H_2 system incorporating demand response," *Energy Convers. Manag.*, vol. 186, pp. 241–257, Apr. 2019.

[43] M. Usman, M. T. Khan, A. S. Rana, and S. Ali, "Techno-economic analysis of hybrid solar-diesel-grid connected power generation system," *J. Elect. Syst. Inf. Technol.*, vol. 5, no. 3, pp. 653–662, 2017.

[44] R. Lingamuthu and R. Mariappan, "Power flow control of grid connected hybrid renewable energy system using hybrid controller with pumped storage," *Int. J. Hydrogen Energy*, vol. 44, no. 7, pp. 3790–3802, 2019.

[45] H. R. Habib and T. Mahmood, "Optimal planning and design of hybrid energy system for UET Taxila," in *Proc. Int. Conf. Elect. Eng. (ICEE)*, 2017, pp. 1–9.

[46] Y. Li, Z. Xu, L. Xiong, G. Song, J. Zhang, D. Qi, and H. Yang, "A cascading power sharing control for microgrid embedded with wind and solar generation," *Renew. Energy*, vol. 132, pp. 846–860, Mar. 2019.

[47] F. Asghar, M. Talha, and S. H. Kim, "Robust frequency and voltage stability control strategy for standalone AC/DC hybrid microgrid," *Energies*, vol. 10, no. 6, p. 760, 2017.

[48] J. Hu, Y. Xu, K. W. Cheng, and J. M. Guerrero, "A model predictive control strategy of PV-battery microgrid under variable power generations and load conditions," *Appl. Energy*, vol. 221, pp. 195–203, Jul. 2018.

[49] X. Lu, K. Sun, J. M. Guerrero, J. C. Vasquez, and L. Huang, "State-of-charge balance using adaptive droop control for distributed energy storage systems in DC microgrid applications," *IEEE Trans. Ind. Electron.*, vol. 61, no. 6, pp. 2804–2815, Jun. 2014.

[50] N. Bizon, "Effective mitigation of the load pulses by controlling the battery/SMES hybrid energy storage system," *Appl. Energy*, vol. 229, pp. 459–473, Nov. 2018.

[51] M. Jayachandran and G. Ravi, "Decentralized model predictive hierarchical control strategy for islanded AC microgrids," *Electr. Power Syst. Res.*, vol. 170, pp. 92–100, May 2019.

[52] M. E. Haque, K. M. Muttaqi, and M. Negnevitsky, "Control of a stand alone variable speed wind turbine with a permanent magnet synchronous generator," in *Proc. IEEE Power Energy Soc. (PES), Gen. Meeting Convers. Del. Elect. Energy 21st Century*, Jul. 2008, pp. 1–9.

[53] *Wind Energy Projects in Pakistan*. Accessed: Apr. 18, 2019. [Online]. Available: http://www.pmd.gov.pk/wind/Wind_Project_files/Page351.html

[54] H. A. Khan, H. F. Ahmad, M. Nasir, M. F. Nadeem, and N. A. Zaffar, "Decentralised electric power delivery for rural electrification in Pakistan," *Energy Policy*, vol. 120, pp. 312–323, Sep. 2018.

[55] O. D. T. Odou, R. Bhandari, and R. Adamou, "Hybrid off-grid renewable power system for sustainable rural electrification in Benin," *Renew. Energy*, vol. 145, pp. 1266–1279, Jan. 2020.

[56] K. Gebrehiwot, M. A. H. Mondal, C. Ringler, and A. G. Gebremeskel, "Optimization and cost-benefit assessment of hybrid power systems for off-grid rural electrification in Ethiopia," *Energy*, vol. 177, pp. 234–246, Jun. 2019.

[57] T. Geyer and D. E. Quevedo, "Performance of multistep finite control set model predictive control for power electronics," *IEEE Trans. Power Electron.*, vol. 30, no. 3, pp. 1633–1644, Mar. 2015.

[58] S. Vazquez, A. Marquez, R. Aguilera, D. Quevedo, J. I. Leon, and L. G. Franquelo, "Predictive optimal switching sequence direct power control for grid-connected power converters," *IEEE Trans. Trans. Ind. Electron.*, vol. 62, no. 4, pp. 2010–2020, Mar. 2015.

[59] T. Dragi ević, "Model predictive control of power converters for robust and fast operation of AC microgrids," *IEEE Trans. Power Electron.*, vol. 33, no. 7, pp. 6304–6317, Jul. 2017.

[60] P. Acuna, L. Moran, M. Rivera, J. Dixon, and J. Rodriguez, "Improved active power filter performance for renewable power generation systems," *IEEE Trans. Power Electron.*, vol. 29, no. 2, pp. 687–694, Feb. 2014.

[61] A. Calle-Prado, S. Alepuz, J. Bordonau, J. Nicolas-Apruzzese, P. Cortés, and J. Rodriguez, "Model predictive current control of grid-connected neutral-point-clamped converters to meet low-voltage ride-through requirements," *IEEE Trans. Ind. Electron.*, vol. 62, no. 3, pp. 1503–1514, Mar. 2015.

[62] P. Acuña, L. Morán, M. Rivera, R. Aguilera, R. Burgos, and V. G. Agelidis, "A single-objective predictive control method for a multivariable single-phase three-level NPC converter-based active power filter," *IEEE Trans. Ind. Electron.*, vol. 62, no. 7, pp. 4598–4607, Jul. 2015.

[63] S. Kouro, P. Cortes, R. Vargas, U. Ammann, and J. Rodriguez, "Model predictive control—A simple and powerful method to control power converters," *IEEE Trans. Ind. Electron.*, vol. 56, no. 6, pp. 1826–1838, Jun. 2009.

[64] C. Xia, T. Liu, T. Shi, and Z. Song, "A simplified finite-control-set model-predictive control for power converters," *IEEE Trans. Ind. Informat.*, vol. 10, no. 2, pp. 991–1002, May 2014.

[65] T. Geyer and D. E. Quevedo, "Multistep finite control set model predictive control for power electronics," *IEEE Trans. Power Electron.*, vol. 29, no. 12, pp. 6836–6846, Dec. 2014.

[66] K. Antoniewicz, M. Jasinski, M. P. Kazmierkowski, and M. Malinowski, "Experimental research on model predictive control of 3-level 4-leg flying capacitor converter operating as shunt active power filter," in *Proc. 41st Annu. Conf. IEEE Ind. Electron. Soc. (IECON)*, Nov. 2015, vol. 63, no. 8, pp. 36–41.

[67] P. Correa, J. Rodriguez, I. Lizama, and D. Andler, "A predictive control scheme for current-source rectifiers," *IEEE Trans. Ind. Electron.*, vol. 56, no. 5, pp. 1813–1815, May 2009.

[68] G. Mirzaeva, G. C. Goodwin, B. P. McGrath, C. Teixeira, and M. E. Rivera, "A generalized MPC framework for the design and comparison of VSI current controllers," *IEEE Trans. Ind. Electron.*, vol. 63, no. 9, pp. 5816–5826, Sep. 2016.

[69] N. Panten, N. Hoffmann, and F. W. Fuchs, "Finite control set model predictive current control for grid-connected voltage-source converters with LCL filters: A study based on different state feedbacks," *IEEE Trans. Power Electron.*, vol. 31, no. 7, pp. 5189–5200, Jul. 2016.

[70] X. Huang, K. Wang, J. Qiu, L. Hang, G. Li, and X. Wang, "Decentralized control of multi-parallel grid-forming DGs in islanded microgrids for enhanced transient performance," *IEEE Access*, vol. 7, pp. 17958–17968, 2019.

HABIB UR RAHMAN HABIB was born in Fort Abbas, Pakistan, in 1988. He received the B.Sc. degree in electrical engineering and the M.Sc. degree in electrical power engineering from the University of Engineering and Technology Taxila, Pakistan, in 2009 and 2015, respectively. He is currently pursuing the Ph.D. degree with the State Key Laboratory of Advanced Electromagnetic Engineering and Technology, Huazhong University of Science and Technology, Wuhan, China. Since 2009, he has been with the COMSATS Institute of Information Technology, Pakistan, and also with the Wah Engineering College, University of Wah, Pakistan. He has been a Management Trainee Officer (Maintenance Department) with Dynamic Packaging Pvt. Ltd., Lahore, Pakistan. He is also permanently with the Department of Electrical Engineering, University of Engineering and Technology Taxila. His research interests include electrical planning and estimation, energy resources and planning, modeling and simulation, renewable energy technology and management, smart grid applications in power system, distributed energy resources and microgrid, algorithm design, and optimization.

SHAORONG WANG received the B.Sc. degree in electrical engineering from Zhejiang University, Hangzhou, China, in 1984, the M.Sc. degree in electrical engineering from North China Electric Power University, China, in 1990, and the Ph.D. degree from the Huazhong University of Science and Technology, China, in 2004, where he is currently a Professor with the School of Electrical and Electronics Engineering. His research interests include smart grid, power system planning, and big data of power systems.

M. R. ELKADEEM received the B.S. and M.S. degrees in electrical engineering from Tanta University, Tanta, Egypt, in 2012 and 2016, respectively. He is currently pursuing the Ph.D. degree with the State Key Laboratory of Advanced Electromagnetic Engineering and Technology, Huazhong University of Science and Technology, Wuhan, China.

He has been working as a Teaching Assistant with the Department of Electrical Power and Machines Engineering, Faculty of Engineering, Tanta University, since 2013. His research interests include distribution automation systems, hybrid renewable energy system planning and design, power system optimization, and reliability analysis.

MAHMOUD F. ELMORSHEDY was born in Gharbeya, Egypt, in 1989. He received the B.Sc. and M.Sc. degrees in electrical engineering from Tanta University, Tanta, Egypt, in 2012 and 2016, respectively. He is currently pursuing the Ph.D. degree with the State Key Laboratory of Advanced Electromagnetic Engineering and Technology, Huazhong University of Science and Technology, Wuhan, China. He has been a Teaching Assistant with the Department of Electrical Power and Machines Engineering, Faculty of Engineering, Tanta University, since 2013, where he was promoted to the degree of Assistant Lecturer, in June 2016. His research interests include linear induction motor, predictive control, power electronics, and renewable energy.